THE DESIGN OF A 3.4 BY 3.4 INCH SUPERSONIC WIND TUNNEL CAPABLE OF CONTINUOUS OPERATION IN THE RANGE OF MACH NUMBERS BETWEEN 1.50 AND 3.59

by

Euell Clay Anderson

Thesis submitted to the Graduate Faculty of the
Virginia Polytechnic Institute
in candidacy for the degree of

MASTER OF SCIENCE

in

AEROSPACE ENGINEERING

December 1962

Blacksburg, Virginia

TABLE OF CONTENTS

LIST OF TABLES AND FIGURES

Tables

Figures

LIST OF SYMBOLS

A	area, square feet
a	constant
b	constant
c	model length, inches
h	tunnel height, inches
M	Mach number
m	mass flow rate, slugs/ft^3
P	pressure, pounds per square inch absolute
R	Reynolds number
T	temperature, degrees Rankine
α	Mach angle
δ	flow deviation through oblique shock, degrees
σ	oblique shock angle, degrees
γ	ratio of specific heats
θ	flow direction, degrees
ω	Prandtl-Meyer angle, degrees
ρ	mass density, slugs/ft^3

Subscripts

E	tunnel exit
M	model cross sectional area
min	minimum
max	maximum

0	stagnation conditions
∞	test section conditions
1	downstream of normal shock

I. INTRODUCTION

To accomplish significant fundamental high speed flow research and adequately demonstrate the variation of fluid properties with increase in Mach number, a high speed wind tunnel with a wider range of Mach numbers is needed to replace the tunnel now used in the Aerospace Engineering Laboratory at the Virginia Polytechnic Institute. Also, the new tunnel should have a test section of sufficient size to permit the use of more realistic test models. The present tunnel, which is capable of producing Mach numbers 1.789 and 1.980 for short periods of time does not adequately demonstrate the variation of aerodynamic properties with increase in Mach number. In addition, the existing tunnel has a test section size of only 0.75 by 1.785 inches; this necessitates the use of extremely small models. Since pressure measurements on models of the size required are very difficult, the tunnel is essentially restricted to experiments permitting the use of optical methods for determining the flow characteristics.

The Mach number range considered in high speed aerodynamic studies is divided into three speed ranges: the transonic range, which encompasses the range of Mach numbers close to one; the supersonic range, the range of Mach numbers between $\sqrt{2}$ and 5; and the hypersonic range, the range of Mach numbers greater than 5. The division into three speed ranges has been brought about by the

experimental difficulties which are associated with each range. In the transonic range, wall interference is the predominating difficulty requiring large ratios of tunnel height to model chord. In the supersonic range, the starting difficulties are not a critical factor and the major consideration is to prevent reflected shocks from impinging on the model. The hypersonic range is generally considered to be the range of Mach numbers in which condensation of air components in the test section is encountered for stagnation temperatures close to atmospheric, a situation which requires heaters to control the temperature.

The Mach number which can be attained in a high speed wind tunnel is determined by the physical characteristics of the nozzle. The requirements of the nozzle are that a desired Mach number be attained in the tunnel test section with the flow parallel to the tunnel axis having constant Mach number distribution across the nozzle exit.

Usually nozzles are made two-dimensional and consist of four main parts (Fig. 1.1): (1) a converging inlet section in which subsonic acceleration occurs; (2) a throat or sonic section; (3) an initial expanding zone in which the flow is rapidly accelerated, with the inclination of the nozzle wall increasing from zero at the throat to the expansion angle at the inflection point; and (4) the straightening part, in which the inclination of the wall decreases from the expansion angle at the inflection point to zero at the nozzle

exit, so that the flow entering the test section is parallel to the tunnel axis, at a given Mach number.

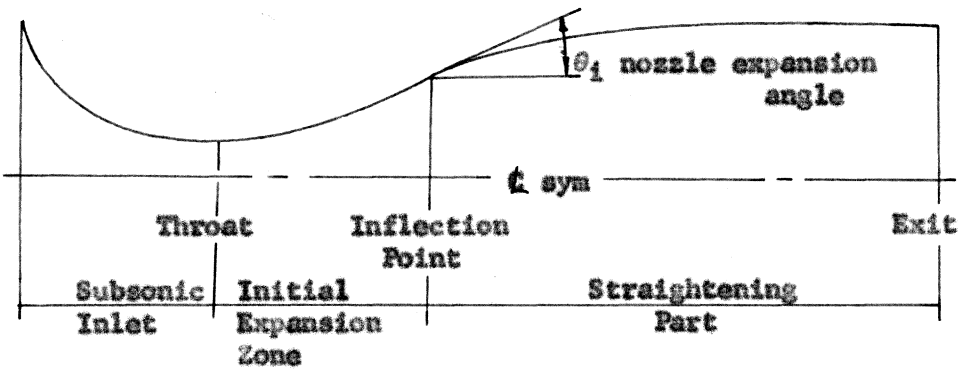

FIGURE 1.1

Supersonic Nozzle Nomenclature

In the two-dimensional nozzle, carefully controlled contours are required on one or at most two walls, the remaining ones being flat. This has the advantage that pressure fluctuations are distributed over the center plane of the tunnel rather than along the axis, as is the case for three-dimensional nozzles. The contour ordinates required to produce the desired flow are determined by the method of characteristics.

Of the several methods available for obtaining variation of Mach number, the two most desirable ones are the flexible nozzle and the fixed-block nozzle. The flexible nozzle, in which flexible plates are supported by jacks positioned along the length of the nozzle and contained between two parallel or slightly diverging sidewalls, is the most versatile. Mach number variation is obtained by adjusting the jacks to predetermined positions; this gives the flexible plate the

required contour for the desired Mach number. Through proper design of the flexible plates and location of the jacks, nearly continuous Mach number variation can be obtained in a given Mach number range. Although the flexible nozzle gives the best combination of versatility and accuracy, the mechanical complexity and high initial cost make this type of nozzle undesirable for a small classroom-type wind tunnel.

The fixed-block nozzle consisting of two identically contoured blocks mounted symmetrically is the most advantageous type for small tunnels, since it is mechanically simple and the initial cost is relatively low. However, in large tunnels the weight of the blocks becomes excessive - special handling equipment is required and the machining difficulties encountered in forming the contours increase the initial cost so that the flexible nozzle is more desirable. The major disadvantage of the fixed-block nozzle is that the Mach number of each block is restricted to a discrete value. Thus, for a change in Mach number, the tunnel must be shut down, and differently contoured blocks must be installed.

For complete simulation of flight conditions the Reynolds number as well as the Mach number of the test model must be the same as that encountered in flight. The Reynolds number range encountered in flight at various altitudes is shown graphically in Fig. 1 as a function of flight Mach number. Since high Mach numbers are usually attained only at high altitudes, a Reynolds number in the range of 10^6 to 10^7 per unit length is generally sufficient to duplicate the flight value.

As can be seen from the following analysis, the Reynolds number of the test section determines the power required to operate the tunnel. The Reynolds number is expressed as

$$R_\infty = \frac{\rho_\infty V_\infty L}{\mu_\infty} \quad , \tag{1.1}$$

where L is the test section dimension. By use of Sutherland's empirical formula for viscosity

$$\mu_\infty = \frac{C_1 T_\infty^{3/2}}{C_2 + T_\infty} \quad , \tag{1.2}$$

the equation of state

$$\frac{P}{\rho} = RT \quad , \tag{1.3}$$

and the definition of Mach number

$$M_\infty = \frac{V_\infty}{a_\infty} \quad , \tag{1.4}$$

the Reynolds number can be expressed as

$$R_\infty = \left[1 + \frac{C_2}{T_\infty}\right] \frac{C_3 M_\infty L P_\infty}{T_\infty} \quad . \tag{1.5}$$

The kinetic energy crossing the test section per unit time is

$$K.E. = \frac{\rho_\infty V_\infty^3 A}{2} = \frac{\rho_\infty V_\infty^3 L^2}{2} \quad , \tag{1.6}$$

where A is the test section area. When the expression for Reynolds

number is introduced, the kinetic energy expression becomes

$$K.E. = \frac{K R_\infty^2 M_\infty T_\infty^{5/2}}{P_\infty \left[1 + \frac{C_2}{T_\infty}\right]^2} \quad . \tag{1.7}$$

Therefore, for a given Mach number and Reynolds number the kinetic energy increases when the static temperature and model size increase, and when the static pressure decreases.

From the above consideration it is seen that the most economical approach to aerodynamic testing is to use small models, high stagnation pressures, and low stagnation temperatures. It is difficult, however, to construct small models or models rigid enough to withstand the aerodynamic loads associated with high stagnation pressures; the possibility, moreover, of condensation of the air components in the test section limits the use of low stagnation temperatures.

Although it is desirable to conduct wind tunnel tests at the flight Reynolds number, the cost of the air supply system generally makes it necessary to conduct tests at Reynolds numbers considerably less than the flight values. A Reynolds number of the order 10^6, based on model length, is considered the minimum value at which test should be conducted.[8]

The results of a preliminary design investigation indicated that a continuous flow supersonic blow-down wind tunnel could be operated in the Mach number range from 1.5 to 3.6. This can be accomplished

without modification to the air supply or test facilities now existing in the Aerospace Engineering Laboratory at the Virginia Polytechnic Institute. The test section dimensions of the continuous flow tunnel would be large enough to permit the use of pressure distribution models of sufficient length to provide Reynolds numbers in excess of the minimum acceptable value of 10^6 (see Fig. 2).

It is, therefore, the purpose of this thesis to suggest a design for a continuous flow supersonic blow-down wind tunnel suitable for student instruction and basic research studies in the Aerospace Engineering Laboratory at the Virginia Polytechnic Institute.

II. DESIGN

The initial steps taken in the design were to determine the Mach number range, from consideration of pressure requirements and existing transonic facilities; it was also necessary to determine the maximum test section area for which the available mass flow is sufficient to operate the tunnel continuously at all design Mach numbers.

The existing air supply system consists of eight two-stage electrically driven reciprocating compressors delivering a total of 3090 cu ft of free air per minute at a pressure of 100 psig. After compression, the air is passed through activated alumina driers where the moisture content is reduced sufficiently to provide air to the tunnel at a dew point of - 40°F at atmospheric pressure. This is sufficient to prevent condensation shocks in the supersonic speed range, but does not preclude the possibility of flow supersaturation at the higher Mach numbers.

The pressure ratio required to start and maintain flow in a supersonic tunnel depends upon the operating Mach number and the efficiency of the diffuser which decelerates the flow from supersonic speed to subsonic. Thus, to obtain optimum performance with a given air supply system or to reduce the power requirements of a tunnel having specific performance characteristics and physical dimensions, an efficient supersonic diffuser should be incorporated into the tunnel design. The diffuser efficiency is generally measured in terms

of the normal shock pressure ratio - the ratio of stagnation pressure ahead of the normal shock at the test section Mach number to that behind the normal shock.

Experimental results obtained with various diffuser shapes[3,4,5] indicate that the operating pressure ratios required with no model in the test section are approximately 1.2 times greater than those predicted by theory for normal shock transition and no subsonic pressure recovery, if simple divergent diffusers are used; they are approximately equal to the theoretical value for normal shock transition and full subsonic pressure recovery, when fixed-geometry convergent-divergent diffusers are used; and they are approximately half this value with variable-throat convergent-divergent diffusers.

With models installed in the test section, the pressure ratios required for starting and maintaining the flow are considerably higher than those for no model. For a tunnel equipped with a variable-throat convergent-divergent diffuser, the pressure ratios required for starting with a model installed are about 1.5 times greater than the theoretical ratio for normal shock transition with full subsonic pressure recovery, and the operating pressure ratios are slightly less than the theoretical values, depending upon the shape, angle of attack, and size of the model.

2.1. Mach Number Range.

Since the tunnel is to be equipped with a variable-throat convergent-divergent diffuser, selection of operating pressure ratios

equal to the theoretical values obtained for normal-shock transition and full subsonic pressure recovery results in conservative estimates of maximum Mach numbers and mass flow rates. The maximum pressure ratio available with the existing air supply is 7.8. Making allowance for the increase in pressure ratio required to start the tunnel, the maximum allowable operating pressure ratio for which starting difficulties will not be encountered is 5.1. Therefore, from Eq. A-5, Appendix A, the upper limit of the Mach number range is found to be M = 3.6.

A Mach number of 1.5 has been selected as the minimum value necessary to obtain Mach number continuity with the existing transonic tunnel, which operates at Mach numbers up to 1.3.

The Mach numbers considered in the subsequent design are 1.50, 2.05, 2.54, 2.91, and 3.59. Since all Mach numbers are within the supersonic range, conventional supersonic wind tunnel design procedures are used for determining the required performance characteristics.

2.2. Test Section Size.

The maximum test section area at each Mach number was determined from continuity for the minimum mass flow condition - minimum operating stagnation pressure. Through use of Eq. A-5, Appendix A, the minimum stagnation pressure, corresponding to the design Mach number and an exit pressure of 14.7 psia, can be determined. The mass flow parameter $\frac{m}{P_o a_o A}$ corresponding to the specific Mach number can

be found from Eq. B-4, Appendix B. If it is assumed that the stagnation temperature is 60°F, the maximum test section areas for which the available mass flow rate of 0.122 slugs/sec is sufficient to maintain continuous operation are:

M	$\left(\frac{P_o}{P_E}\right)_{min}$	P_o min psia	$P_o \times 10^3$ slugs/ft^3	a_o ft/sec	$\frac{m}{P_o a_o A}$	A ft^2
1.50	1.15	16.90	2.73	1117	0.500	0.0802
2.05	1.39	20.40	3.30	1117	0.344	0.0922
2.54	2.01	29.40	4.66	1117	0.220	0.1065
2.91	2.80	41.10	6.66	1117	0.151	0.1090
3.59	5.10	75.00	11.62	1117	0.078	0.1210

TABLE 2.1

To minimize construction cost and reduce the complexity of the variable-throat diffuser, it was essential to make all nozzles with the same exit dimensions. Therefore, the maximum allowable test section area is determined by the conditions at M = 1.50. From consideration of the requirements for conducting tests with axially symmetric models, it was decided that the tunnel should have a square test section resulting in the dimensions 3.40 by 3.40 inches.

The test section has been provided with optical quality glass windows with dimensions of 3.40 by 6.00 inches to permit observation of the test flow region. The windows are easily removed for model

installation and inspection. The test section components are given in Table 2.1.

In the downstream end of the test section, a sting model mount (see Table 2.1) has been provided. Angles of attack between - 10° and + 10° can be obtained, and the position of the models can be varied with respect to the tunnel's vertical axis.

2.3. Model Requirements.

In order to obtain satisfactory experimental results and tunnel operation, the model must meet the following requirements: (1) the ratio of model area to test section area, $\frac{A_M}{A}$, must be equal to or less than the value obtained from Eq. C-7, Appendix C, for the normal shock, which occurs during the starting process, to pass downstream of the test section; and (2) the model length must be within the limits obtained from Eq. C-8, Appendix C, to prevent model shock wave interaction.

Where the ratios of $\left(\frac{A_M}{A}\right)_{min}$ of Eq. C-7 have been converted to tunnel height model chord ratios for two-dimensional test bodies having a thickness ratio of 0.12, the results obtained from Eqs. C-7 and C-8 at the specified design Mach numbers are:

M	Equation C-7			Equation C-8	
	$(\frac{A_M}{A})_{min}$	$(h/c)_{min}$	c_{max} (inches)	$(h/c)_{min}$	c_{max} (inches)
1.50	0.080	1.50	2.27	1.41	2.40
2.05	0.171	0.70	4.85	1.01	3.37
2.54	0.241	0.50	6.80	0.84	4.05
2.91	0.275	0.43	7.90	0.80	4.25
3.59	0.313	0.38	9.00	0.80	4.25

TABLE 2.2

From the above results, it is seen that the model chord which can be used is determined by the model shock wave interaction requirements for all Mach numbers except at M = 1.50. If, however, the model thickness ratio is less than 0.11, the maximum model length is determined by Eq. C-8 for all Mach numbers considered.

2.4. Reynolds Number.

With the minimum and maximum values of P_o for which the tunnel will operate continuously at the design Mach numbers, the Reynolds number variation can be determined from Fig. 2. The maximum values of P_o have been determined from mass flow continuity considerations. The results obtained for model lengths of 2.40, 3.37, 4.05, and 4.25 inches are:

M	P_o psia		$\frac{R_\infty}{P_o C}$	$R_\infty \times 10^{-6}$ C=2.40 inches		$R_\infty \times 10^{-6}$ C=3.37		$R_\infty \times 10^{-6}$ C=4.05		$R_\infty \times 10^{-6}$ C=4.25	
	Min	Max		Min	Max	Min	Max	Min	Max	Min	Max
1.50	16.90	16.90	28.00	1.13	1.13	-	-	-	-	-	-
2.05	20.40	23.40	23.50	1.17	1.34	1.65	1.88	-	-	-	-
2.54	29.40	39.00	18.30	1.29	1.72	1.82	2.42	2.08	2.90	-	-
2.91	41.10	55.70	15.00	1.48	2.01	2.08	2.84	2.50	3.41	2.62	3.56
3.59	75.00	113.50	10.50	1.89	2.85	2.65	4.00	3.19	4.80	3.35	5.05

TABLE 2.3

From the results tabulated in Table 2.3, it is seen that the minimum Reynolds number for all test Mach numbers exceeds the minimum acceptable value of 1×10^6 if models 2.40 inches long or longer are used. To obtain higher test Reynolds numbers, the tunnel can be operated as an intermittent blow-down tunnel. Through the utilization of the auxiliary air compressor station, which provides stagnation pressures of up to 150 psig, Reynolds numbers up to 7.5×10^6 can be obtained with a model length of 2.40 inches.

2.5. Nozzle.

The designing of a supersonic nozzle generally involves determining the nozzle contour by the method of characteristics based on isentropic perfect fluid flow, calculating the rate of boundary layer growth along the nozzle walls, and making corrections to the nozzle contour to compensate for the boundary layer thickness. For nozzles of the length used in this tunnel, it was found that the corrections for boundary layer growth were of the same order of magnitude as the machining errors. Therefore, it is not necessary to correct for boundary layer effects. Since the method of characteristics as outlined in Appendix D is not applicable to subsonic flows, a starting point must be assumed in a region where the flow speed is equal to, or greater than the speed of sound. Puckett's[6,7] semi-graphical method of determining the nozzle contour is based on the assumption that the flow adjusts itself at the throat so that the flow is sonic

and parallel to the tunnel axis along a perpendicular line at the minimum section. In the use of this method, the graphic solution of the relevant equations represents the curve of the nozzle from the throat section on, an arbitrary curve being used for the initial expansive portion; an alternative procedure is to determine the entire nozzle contour by initiating the solution from a desired Mach number distribution along the tunnel center plane.

In order to have a net increase in flow area without any net change in flow direction, it is necessary that the nozzle curve outward from the throat to the inflection point and then curve inward until at the nozzle exit the contour is parallel to the tunnel axis. At the inflection point the nozzle contour has its maximum slope θ_i, the nozzle expansion angle. As has been discussed in Appendix D, the Prandtl-Meyer angle, ω, is increased by the amount $\Delta\theta$ when the flow crosses an expansion wave. Therefore, the number of Mach waves separating the initial and final flow regions determines the magnitude of the nozzle expansion angle θ_i.

The number of expansion waves separating the initial and final flow regions is[13]

$$N = n(2n_r + 2) \quad , \qquad (2.1)$$

where N is the number of expansion waves, n the number of Mach waves originating along the initial expansion section of the nozzle, and n_r the number of times each wave is reflected before calcellation. If all

the segments of the initial curve differ in inclination by a constant amount $\Delta\theta$ then the Prandtl-Meyer angle is related to N and $\Delta\theta$ by

$$\omega_\infty = N\,\Delta\theta\ , \tag{2.2}$$

and since $\theta_i = n\,\Delta\theta$, the nozzle expansion angle is related to the Prandtl-Meyer angle by the equation

$$\theta_i = \frac{\omega_\infty}{2(n_r + 1)}\ . \tag{2.3}$$

The same result as given by Eq. 2.3 is obtained if $\Delta\theta$ does not have a constant value. In this case,

$$\omega_\infty = n_1(2n_r + 2)\,\Delta\theta_1 + n_2(2n_r + 2)\,\Delta\,\theta_1 + \ldots + , \tag{2.4}$$

where n_1 is the number of waves originating from the initial expansion segments with an increase in inclination at $\Delta\ \theta_1$, and n_2 the number of waves originating from segments with an increase in inclination of $\Delta\ \theta_2$, etc. Since $\theta_i = n_1\ \Delta\ \theta_1 + n_2\ \Delta\ \theta_2 + \ldots +$, the result is the same as given by Eq. 2.3. From the results of Eq. 2.3, it is seen that values of $\theta_i \quad \frac{\omega_\infty}{2}$ are required to avoid a recontraction in the nozzle contour.

The semi-graphical method developed by Puckett has been employed in determining all the nozzle contours. The advantage of this method is that accurate graphical construction is necessary in the physical plane only. The flow direction, Mach number, and Prandtl-Meyer angle in each flow region are given by the numerical constants a and b (Eqs. D-23 and D-24, Appendix D).

The procedure followed in the determination of the nozzle contours by the semi-graphical method is as follows:

(1) Determine the throat height required from the one-dimensional area - Mach number relation given by Eq. B-2, Appendix B, and the nozzle-exit height.

(2) Determine the Prandtl-Meyer angle, corresponding to the design Mach number, by use of Eq. D-22, Appendix D.

(3) Using Eq. 2.3, determine the nozzle expansion angle θ_i.

(4) Starting at the throat, construct an arbitrary initial curve and divide into small straight segments with the inclinations increasing from 0^o at the throat to θ_i at the inflection point.

(5) Prepare a rough sketch of the nozzle and Mach waves dividing the nozzle into regions of uniform flow. Since only expansion waves occur in a nozzle, the values of the constants a and b in each region can be readily determined.

(6) With the values of a and b, determine the flow direction θ, Mach number M, the Prandtl-Meyer angle ω, and the Mach angle α for each flow region.

(7) Construct the Mach lines in the physical plane at the average Mach angle corresponding to the Mach numbers in the flow regions separated by the wave.

(8) Define the nozzle contour by constructing a smooth curve approximating the straight segments obtained with the graphical construction for the supersonic portion - the subsonic inlet portion can be defined by a circular arc or any other smooth curve.

(9) Check the accuracy of the graphical construction against the one-dimensional area-Mach number requirement.

The semi-graphical procedure as outlined above is demonstrated by the following example for a free-stream Mach number of 1.50.

From Fig. 5 the ratio $\frac{A}{A^*}$ corresponding to a Mach number of 1.50 is 1.178. For a two-dimensional nozzle with straight side walls, the ratio $\frac{A}{A^*}$ is equal to the ratio of nozzle-exit height to nozzle throat height $\frac{h}{h^*}$. Therefore, for a nozzle-exit height of 3.400 inches the required throat height is 1.443 inches.

The Prandtl-Meyer angle corresponding to a Mach number of 1150 is 12.0°, and for one reflection of each expansion wave, the nozzle expansion angle θ_i is 3.0°. The arbitrary initial curve is constructed and divided into straight segments having successive increases in inclination of $\Delta\theta = 1^\circ$.

A sketch of the Mach wave pattern is then made (Fig. 2.2) and the values of a and b are determined. The constant a increases by an amount $\Delta\theta$ when the flow crosses a right-running Mach wave, but is unchanged when a left-running wave is crossed. The constant b,

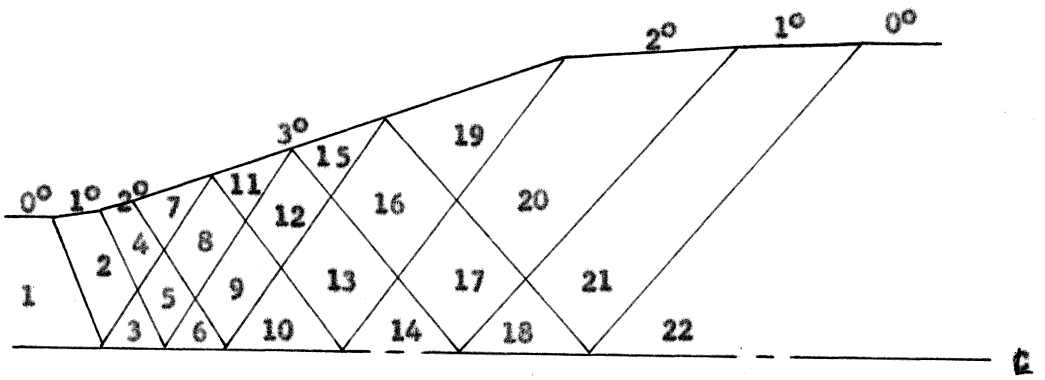

FIGURE 2.1

Sketch of Mach Waves

on the other hand, increases by $\Delta\theta$ when the flow crosses a left-running wave, but is unchanged when right-running waves are crossed. The constants a and b for each region of flow can be readily determined, therefore, with the aid of the sketch. The values of a and b for the resulting flow regions are:

Region	1	2	3	4	5	6	7	8	9	10	11	12	13	14	15	16	17	18	19	20	21	22
a	0	1	1	2	2	2	3	3	3	3	4	4	4	4	5	5	5	5	6	6	6	6
b	0	0	1	0	1	2	0	1	2	3	1	2	3	4	2	3	4	5	3	4	5	6

TABLE 2.4

From the above results and the tables of ω, M, and α given in reference 7, the graphical construction in the physical plane can be performed. In region 1

$$\theta_1 = a_1 - b_1 = 0$$

and

$$\omega_1 = a_1 + b_1 = 0$$

and corresponding to $\omega_1 = 0$, the tables of reference 7 give $M_1 = 1.00$ and $\alpha_1 = 90.00^\circ$. In region 2

$$\theta_2 = a_2 - b_2 = 1 - 0 = 1^\circ$$

and

$$\omega_2 = a_2 + b_2 = 1 + 0 = 1^\circ$$

and corresponding to $\omega_2 = 1^\circ$, $M_2 = 1.0808$, and $\alpha_2 = 67.70^\circ$. Thus, $\beta_{1,2}$ the inclination of the expansion wave separating regions 1 and 2, is

$$\beta_{1,2} = \frac{\theta_1 + \theta_2}{2} - \frac{\alpha_1 + \alpha_2}{2} = \frac{0 + 1}{2} - \frac{90.00 + 67.70}{2} = -78.5^\circ$$

By a similar procedure, the inclination of the expansion wave separating regions 2 and 3 is found to be

$$\beta_{2,3} = \frac{\theta_2 + \theta_3}{2} + \frac{\alpha_2 + \alpha_3}{2} = \frac{1 + 0}{2} + \frac{67.70 + 61.96}{2} = 65.33^\circ \quad .$$

The nozzle coordinates resulting from the graphical construction at Mach numbers of 1.50, 2.05, 2.54, 2.91, and 3.59, are given in Table 2.

2.6. Diffuser.

The purpose of the diffuser is to reduce the free stream Mach number through a series of oblique shock waves so that the normal shock transition occurs at a lower Mach number. Since the losses in pressure across oblique shock waves are much less than that across a normal shock at the same Mach number, an appreciable increase in pressure recovery is obtained. Therefore, the pressure ratio, mass flow, and power required to operate a tunnel at a given free stream

Mach number are reduced by the use of a diffuser. As the number of oblique shocks occurring in the convergent portion of the diffuser become large, the diffuser efficiency approaches that of isentropic pressure recovery. However, a large number of oblique shocks requires a long diffuser and the losses associated with the boundary layer become large.

The diffuser efficiency is also dependent upon the configuration of the model and model mount, boundary layer shock wave interaction, and the divergence angle of the subsonic portion of the diffuser. The losses associated with these effects vary with the test section Mach number and generally cannot be estimated by theoretical methods.

Therefore, the diffuser (see Table 1) was designed to function theoretically as a double oblique shock wedge type diffuser with a perfect fluid at an intermediate Mach number of 2.50, under which circumstances it would, of course, obtain the theoretical maximum pressure recovery.

When the tunnel is started, the diffuser throat area, A_{*1}, must be sufficient to permit the starting normal shock to pass downstream of the throat. The magnitude of A_{*1}, to permit starting, corresponds to $(A - A_M)$ given by Eq. C-7, Appendix C. After the supersonic flow is established, the diffuser throat area is reduced to the most efficient value, which is determined experimentally for each model configuration.

III. CONCLUDING REMARKS AND RECOMMENDATIONS

The addition of the tunnel designed will provide adequate test facilities for student instruction and basic research studies in both the transonic and supersonic range of Mach numbers, when used in conjunction with the existing test facilities in the Aerospace Engineering Laboratory at VPI. A tunnel of the type designed may be used for studying stability and control problems of practical body shapes, and boundary layer stability and skin friction studies for zero heat transfer conditions are made possible with a continuous flow tunnel. Supersonic inlet duct research studies will be greatly facilitated, and by the addition of an air heating system, heat transfer problems and the effect of such variables as angle of attack, interfering flow fields, and separated flow regions, both with and without cooling, can be studied experimentally.

It is, therefore, recommended that the supersonic wind tunnel designed be constructed and installed in the Aerospace Engineering Laboratory at Virginia Polytechnic Institute, and that provisions for controlling the stagnation temperature of the air be incorporated into the air supply system.

IV. SUMMARY

The design of a 3.4 by 3.4-inch supersonic wind tunnel to be used in the Aerospace Engineering Laboratory at the Virginia Polytechnic Institute is described. The purpose of the design is to provide adequate facilities for instructional and basic supersonic flow research. The tunnel is of the continuous blow-down non-return type discharging directly to the atmosphere.

Two-dimensional, symmetric, fixed block nozzles have been designed to provide test Mach numbers of 1.50, 2.05, 2.54, 2.91, and 3.59. Reynolds numbers of 1.1×10^6 to 5.0×10^6 can be obtained, depending upon the Mach number and model length. Higher test Reynolds numbers are possible by intermittent operation of the tunnel.

V. ACKNOWLEDGEMENTS

The author wishes to express his appreciation to Professors and for their suggestions and assistance in the preparation of this thesis.

The author also wishes to thank for the typing of this thesis.

VI. BIBLIOGRAPHY

1. The Staff of the Ames 1- by 3-foot Supersonic Wind Tunnel Section, NOTES AND TABLES FOR USE IN THE ANALYSIS OF SUPERSONIC FLOW. NACA TN 1428, 1947.

2. Leavey, L. E., A SUPERSONIC WIND TUNNEL FOR MACH NUMBERS UP TO 3.5. Advisory Group for Aeronautical Research and Development, Report 70, 1956.

3. Diggins, J. L., DIFFUSER INVESTIGATION IN A SUPERSONIC WIND TUNNEL. NAVORD Report 1570, 1951.

4. Neumann, E. P. and Lustwick, F., SUPERSONIC DIFFUSERS FOR WIND TUNNELS. Journal Applied Mechanics, Vol. 16, No. 2, 1949.

5. Neumann, E. P. and Lustwick, F., HIGH EFFICIENCY SUPERSONIC DIFFUSERS. Journal of Aeronautical Sciences, Vol. 18, No. 6, 1951.

6. Puckett, A. E., SUPERSONIC NOZZLE DESIGN, Journal Applied Mechanics, Dec. 1946.

7. Puckett, A. E., DESIGN AND OPERATION OF A 12-INCH SUPERSONIC WIND TUNNEL. Institute of Aeronautical Sciences, Preprint No. 160, 1948.

8. Lindsey, W. F. and Crew, W. L., THE DEVELOPMENT AND PERFORMANCE OF TWO SMALL TUNNELS CAPABLE OF INTERMITTENT OPERATION AT MACH NUMBERS BETWEEN 0.4 AND 4.0. NACA TN 2189, 1950.

9. Ackert, J., HIGH SPEED WIND TUNNELS, NACA TM 808, 1936.

10. Telervin, Neal, APPROXIMATE FORMULAS FOR THE COMPUTATION OF TURBULENT BOUNDARY-LAYER MOMENTUM THICKNESSES IN COMPRESSIBLE FLOWS. NACA ACR L6A22, 1946.

11. Tucker, Maurice, APPROXIMATE TURBULENT BOUNDARY-LAYER DEVELOPMENT IN PLANE COMPRESSIBLE FLOW ALONG THERMALLY INSULATED SURFACES WITH APPLICATION TO SUPERSONIC TUNNEL CONTOUR CORRECTION. NACA TN 2045, 1950.

12. Kantrowitz, Arthur, and Donaldsen, Coleman duP., PRELIMINARY INVESTIGATION OF SUPERSONIC DIFFUSERS. NACA ACR L5D20, 1945.

13. Ruptash, J., SUPERSONIC WIND TUNNELS - THEORY, DESIGN AND PERFORMANCE. UTIA Review No. 5, June, 1952.

The vita has been removed from the scanned document

VIII. APPENDICES

APPENDIX A

Pressure Required to Maintain Supersonic Flow

The pressure ratio required to maintain a supersonic flow field in the wind tunnel test section can be closely estimated by considering the pressure losses across a normal shock at the test section Mach number. The two possibilities for the pressure ratio required for normal shock transition from supersonic to subsonic flow are: (1) no subsonic pressure recovery after the normal shock, and (2) full subsonic pressure recovery.

For the case of normal shock transition with no subsonic recovery (Fig. A-1), the pressure ratio required is the product of the isentropic pressure relation upstream of the shock and the pressure relation across the normal shock.

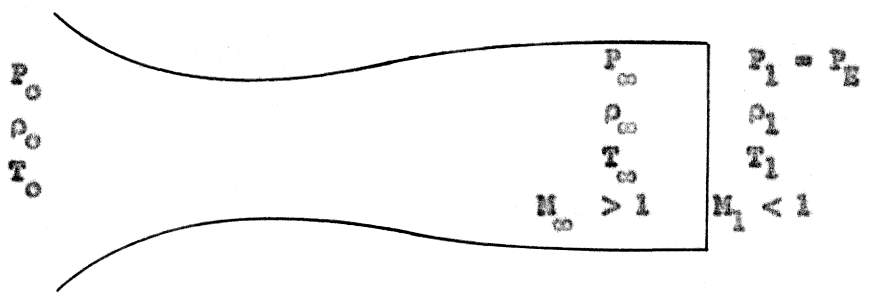

FIGURE A-1

Normal Shock Transition and No Subsonic Pressure Recovery

The pressure ratio between the stagnation chamber and the test section is given by

$$\frac{P_o}{P_\infty} = \left[1 + \frac{\gamma - 1}{2} M_\infty^2\right]^{\frac{\gamma}{\gamma - 1}}, \qquad \text{(A-1)}$$

and across the normal shock the pressure ratio is

$$\frac{P_\infty}{P_1} = \frac{\gamma + 1}{2\gamma M_\infty^2 - (\gamma - 1)} \qquad \text{(A-2)}$$

Since for no subsonic pressure recovery $P_1 = P_E$, the required pressure ratio is given by

$$\frac{P_o}{P_E} = \frac{P_o}{P_1} = \left[1 + \frac{\gamma - 1}{2} M_\infty^2\right]^{\frac{\gamma}{\gamma - 1}} \left[\frac{\gamma + 1}{2\gamma M_\infty^2 - (\gamma - 1)}\right]. \qquad \text{(A-3)}$$

For full subsonic recovery (Fig. C-2), the flow is isentropic on the upstream and downstream sides of the normal shock.

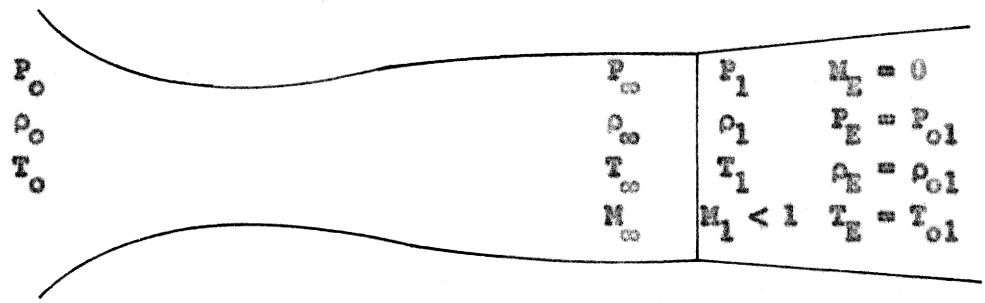

FIGURE A-2

Normal Shock Transition and Full Subsonic Pressure Recovery

The isentropic pressure relation downstream of the normal shock, in terms of the free stream Mach number, is

$$\frac{P_1}{P_E} = \frac{P_1}{P_{01}} = \left[1 + \frac{\gamma - 1}{2}\left(\frac{(\gamma - 1) M_\infty^2 - 2}{2\gamma M_\infty^2 - (\gamma - 1)}\right)\right]^{-\frac{\gamma}{\gamma - 1}} \qquad \text{(A-4)}$$

The product of Eqs. A-1, A-2, and A-4 gives the required pressure ratio in terms of M_∞ as

$$\frac{P_o}{P_E} = \left[\frac{2 + (\gamma - 1) M_\infty^2}{(\gamma - 1) M_\infty^2}\right]^{\frac{\gamma}{\gamma - 1}} \left[\frac{2\gamma M_\infty^2 - (\gamma - 1)}{\gamma + 1}\right]^{\frac{\gamma}{\gamma - 1}} \qquad \text{(A-5)}$$

Equations A-3 and A-5 are represented graphically in Fig. 4.

APPENDIX B

Area Ratio and Mass Flow Requirements

The flow at the nozzle throat and exit sections is one-dimensional. Thus, a dimensionless area ratio expressed in terms of the free stream Mach number can be obtained. The continuity equation

$$\rho_* \, a_* \, A_* = \rho_\infty \, a_\infty \, A \quad , \tag{B-1}$$

and the isentropic relations

$$\rho_o = \rho_\infty \left(1 + \frac{\gamma - 1}{2} M_\infty^2\right)^{\frac{1}{\gamma - 1}} , \quad \rho_* = \rho_o \left(\frac{2}{\gamma + 1}\right)^{\frac{1}{\gamma - 1}}$$

$$a_o = a_\infty \left(1 + \frac{\gamma - 1}{2} M_\infty^2\right)^{1/2} , \text{ and } \quad a_* = a_o \left(\frac{2}{\gamma + 1}\right)^{1/2}$$

gives

$$\frac{A_*}{A} = M_\infty \left[\frac{\gamma + 1}{2 + (\gamma - 1) M_\infty^2}\right]^{\frac{\gamma + 1}{2(\gamma - 1)}} . \tag{B-2}$$

The ratio $\frac{A_*}{A}$ is always less than unity for values of $M_\infty \neq 1$, and for any given ratio $\frac{A_*}{A} < 1$ there are two values of M_∞ which satisfy Eq. B-2 - one being subsonic and the other supersonic.

By a similar analysis, a dimensionless mass flow parameter can be expressed as

$$\frac{m}{P_o \, a_o \, A_*} = \left(\frac{2}{\gamma + 1}\right)^{\frac{\gamma + 1}{2(\gamma - 1)}} \tag{B-3}$$

or for $\gamma = 1.4$

$$\frac{\dot{m}}{P_o\, a_o\, A} = 0.578\, \frac{A_*}{A} \quad . \tag{B-4}$$

Equations B-2 and B-3 are represented graphically in Fig. 5.

APPENDIX C

Tunnel Height - Model Chord Ratio Requirements

The maximum ratio of model cross-sectional area to test section area which will permit starting of the tunnel can be determined by assuming that the normal shock during the starting process stands ahead of the model. Then the minimum value of the reduced area, caused by the presence of the model, will correspond to sonic conditions behind the normal shock.

For sonic flow in the reduced area (see Fig. C-1), the continuity equation requires

$$\rho_x \, a_x \, A_* = \rho_{x1} \, a_{*1} (A - A_M) \quad . \tag{C-1}$$

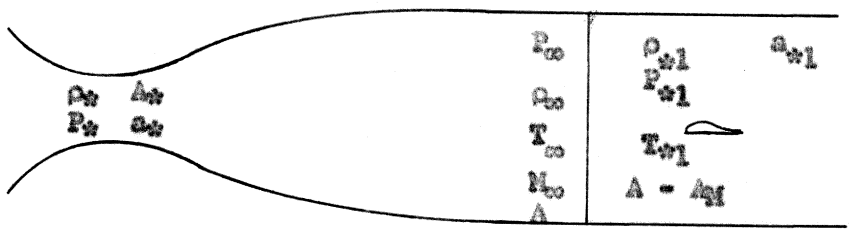

FIGURE C-1
Nomenclature

The energy equation for adiabatic flow

$$C_p T + \frac{V^2}{2} = C_p \, T_o$$

or

$$\frac{\gamma}{\gamma - 1} \frac{P}{\rho} + \frac{V^2}{2} = \frac{\gamma}{\gamma - 1} \frac{P_o}{\rho_o} \tag{C-2}$$

with $M_* = M_{*1} = 1$ requires

$$\frac{P_*}{\rho_*} = \frac{P_{*1}}{\rho_{*1}} \quad \text{or} \quad a_* = a_{*1} \quad , \tag{C-3}$$

and

$$\frac{P_o}{\rho_o} = \frac{P_{o1}}{\rho_{o1}} \tag{C-4}$$

Since the flow is assumed to be isentropic before and after the normal shock, the density ratios are

$$\frac{\rho_*}{\rho_o} = \frac{\rho_{*1}}{\rho_{o1}} = \left(\frac{2}{\gamma + 1} \right)^{\frac{1}{\gamma - 1}} \quad . \tag{C-5}$$

From relations C-1 to C-5 it is seen that

$$\left(\frac{A - A_M}{A} \right) \leq \frac{P_{o1}}{P_o} \tag{C-6}$$

is required to permit the normal shock to pass downstream of the model and therefore to establish supersonic flow in the test section.

Expressing Eq. C-6 in terms of the test section area and free stream Mach number gives

$$\left(\frac{A-A_M}{A} \right)_{min} = \left(\frac{2}{\gamma + 1} \right)^{\frac{\gamma+1}{2(\gamma-1)}} \frac{\left(\gamma M_\infty^2 - \frac{\gamma-1}{2} \right)^{\frac{1}{\gamma-1}} \left(1 + \frac{\gamma-1}{2} M_\infty^2 \right)^{1/2}}{M_\infty \frac{\gamma + 1}{\gamma - 1}} \tag{C-7a}$$

or

$$\left(\frac{A_M}{A}\right)_{max} = 1 - \left(\frac{2}{\gamma+1}\right)^{\frac{\gamma+1}{2(\gamma-1)}} \frac{\gamma M_\infty^2 - \left(\frac{\gamma-1}{2}\right)^{\frac{1}{\gamma-1}} \left(1 + \frac{\gamma-1}{2} M_\infty^2\right)^{1/2}}{M_\infty \frac{\gamma+1}{\gamma-1}} \qquad \text{(C-7b)}$$

Equations C-7 are represented graphically in Fig.

For two-dimensional tests with bodies of a given thickness ratio the results of Eqs. B-7 can be converted to tunnel height model chord ratios.

The values of h/c determined from Eqs. C-7 are usually less than that required to prevent reflected shocks from impinging on the tracking edge of the model[8]. The exception being when tests are conducted with bodies of very large thickness ratios.

To prevent reflected shock interference, the minimum value of h/c can be determined by considering a flat plate at the maximum angle of attack for which supersonic flow throughout the test section is retained. From trigometric relations and the shock properties, σ_1 the initial shock angle, σ_2 the reflected shock angle, and δ the flow deviation, the minimum value of h/c is

$$(h/c)_{min} = \frac{2 \tan \sigma_1 \tan (\sigma_2 - \delta)}{\tan \sigma_1 + \tan (\sigma_2 - \delta)} \quad . \qquad \text{(C-8)}$$

where the values of σ_1, σ_2, and δ are obtained from reference 1. The results of Eq. C-8 are somewhat conservative when compared with the values given in reference 2.

APPENDIX D

Method of Characteristics

The equations of motion describing a compressible fluid in two or three dimensions are generally non-linear, since the dependent variables and their derivatives appear as products. The non-linearity of these equations makes them difficult to solve by analytical means without making severe simplifying assumptions - with the exception of a few simple cases. In the special case where the speed is everywhere supersonic, the equations of motion become hyperbolic in nature and can be solved by the method of characteristics. Since the conventional methods of designing supersonic nozzles - both two-dimensional and axially symmetric - usually involve the use of characteristics, an outline of the method is presented. It is assumed that the fluid in a perfect gas having no viscosity, thermal conductivity, and no discontinuities - such as those associated with shock waves - are present.

Two-Dimensional Isentropic Steady Flow.

The equations governing the motion of a two-dimensional, steady flow, irrotational, non-viscous, compressible fluid are given by

$$(a^2 - u^2)\frac{\partial u}{\partial x} + uv\left(\frac{\partial u}{\partial x} + \frac{\partial v}{\partial y}\right) + (a^2 - u^2)\frac{\partial v}{\partial y} = 0 \qquad \text{(D-1)}$$

derived from Euler's equation and the equation of continuity, and

$$\frac{\partial u}{\partial y} - \frac{\partial v}{\partial x} = 0 \qquad \text{(D-2)}$$

which expresses the condition of irrotationality.

In the derivation of the characteristic equations, it is assumed that u and v are defined for all points (x,y) along a curve C in the x-y plane. Letting s specify position along the curve C, the equation of the curve C can be represented by

$$\begin{aligned} x &= x(s) \\ y &= y(s) \end{aligned} \qquad \text{(D-3)}$$

For points on C the dependent variables (u,v) are considered to be prescribed functions of s. Assuming that u and v can be expanded in a power series of the form

$$u(x,y) = u(x_o,y_o) + \sum_{n=1}^{\infty} \frac{1}{N!} \left[(x-x_o) \frac{\partial}{\partial x} + (y-y_o) \frac{\partial}{\partial y} \right]^n u$$

$$v(x,y) = v(x_o,y_o) + \sum_{n=1}^{\infty} \frac{1}{N.} \left[(x-x_o) \frac{\partial}{\partial x} + (y-y_o) \frac{\partial}{\partial y} \right]^n v$$

about a point (x_o,y_o) on C, then knowing u and v along the curve C as functions of s their derivatives can be calculated along C and must satisfy the equations

$$\frac{du}{ds} = \frac{\partial u}{\partial x} \frac{dx}{ds} + \frac{\partial u}{\partial y} \frac{dy}{ds} \quad . \qquad \text{(D-4)}$$

and

$$\frac{dv}{ds} = \frac{\partial v}{\partial x}\frac{dx}{ds} + \frac{\partial v}{\partial y}\frac{dy}{ds} \quad . \tag{D-5}$$

The initial step in determining u(x,y), is to evaluate the derivatives $\left(\frac{\partial u}{\partial x}\right)_{x_o,y_o}$, $\left(\frac{\partial u}{\partial y}\right)_{x_o,y_o}$, and similarily for determining v(x,y). The derivatives $\frac{\partial u}{\partial x}$, $\frac{\partial u}{\partial y}$, $\frac{\partial v}{\partial x}$, and $\frac{\partial v}{\partial y}$ are determined from the four equations A-1, A-2, A-4 and A-5 which may be expressed as

$$\begin{aligned}
&(a^2 - u^2)\frac{\partial u}{\partial x} - uv\frac{\partial u}{\partial y} - uv\frac{\partial v}{\partial x} + (a^2 - u^2)\frac{\partial v}{\partial y} = 0 \\
&0 \qquad\qquad \frac{\partial u}{\partial y} - \frac{\partial v}{\partial x} \qquad 0 \qquad = 0 \\
&\frac{dx}{ds}\frac{\partial u}{\partial x} + \frac{dy}{ds}\frac{\partial u}{\partial y} \qquad 0 \qquad 0 \qquad = 0 \\
&0 \qquad\qquad 0 + \frac{dx}{ds}\frac{\partial v}{\partial x} + \frac{dy}{ds}\frac{\partial v}{\partial y} = 0 \quad .
\end{aligned} \tag{D-6}$$

Let D represent the determinant of coefficients and D_n the determinant obtained by substituting the right-hand side of D-6 for the nth column. Then

$$\frac{\partial u}{\partial x} = \frac{D_1}{D}, \quad \frac{\partial u}{\partial y} = \frac{D_2}{D}, \quad \frac{\partial v}{\partial x} = \frac{D_3}{D}, \text{ and } \frac{\partial v}{\partial y} = \frac{D_4}{D} \quad .$$

If D = 0 there are two possibilities:

(1) $D_n \neq 0$

In this case, the system of equations is inconsistent.

(2) $D_n = 0$

In this case, the system of equations is consistent.

In case (1) there is no solution, and in case (2) there are a number of solutions but no unique solution. If $D \neq 0$ a unique solution is obtained.

The necessary and sufficient condition for the existence of a characteristic solution is $D = 0$ and all D_n's $= 0$. The requirement $D = 0$ is referred to as the characteristic condition, and $D_n = 0$ is referred to as the compatibility condition.

In Eq. D-6 the characteristic condition requires

$$D = \begin{vmatrix} (a^2 - u^2) & -uv & -uv & (a^2 - u^2) \\ 0 & 1 & -1 & 0 \\ \frac{dx}{ds} & \frac{dy}{ds} & 0 & 0 \\ 0 & 0 & \frac{dx}{ds} & \frac{dy}{ds} \end{vmatrix} = 0 \qquad \text{(D-7)}$$

By expansion, this equation can be written in the form

$$(a^2 - u^2)\left(\frac{dx}{ds}\right)^2 + 2uv\,\frac{dx}{ds}\,\frac{dy}{ds} + (a^2 - u^2)\left(\frac{dy}{ds}\right)^2 = 0 \qquad \text{(D-8)}$$

or

$$\frac{dy}{dx} = \frac{-uv \pm a\sqrt{v^2 - a^2}}{a^2 - u^2}$$

where $V^2 = u^2 + v^2$. The compatibility condition requires

$$D_4 = \begin{vmatrix} (a^2 - u^2) & -uv & -uv & 0 \\ 0 & 1 & -1 & 0 \\ \frac{dx}{ds} & \frac{dy}{ds} & 0 & \frac{du}{ds} \\ 0 & 0 & \frac{dx}{ds} & \frac{dv}{ds} \end{vmatrix} = 0 \qquad \text{(D-9)}$$

Expanding Eq. D-9 gives

$$(a^2 - u^2)\left(\frac{du}{ds}\frac{dx}{ds} - \frac{dv}{ds}\frac{dy}{ds}\right) - 2uv\,\frac{dv}{ds}\frac{dy}{ds} = 0 \qquad \text{(D-10)}$$

or

$$\frac{du}{dv} = \frac{dy}{dx} + \frac{2uv}{a^2 - u^2} = \frac{uv \pm a\sqrt{V^2 - a^2}}{a^2 - u^2}$$

If $V > a$, supersonic flow, the system of Eqs. D-1 and D-2, is hyperbolic and consequently Eqs. A-8 and A-10 have two real roots and two characteristic directions. If $V < a$, subsonic flow, the system of equations is elliptic, and the roots of Eqs. D-8 and D-10 are imaginary. If $V = a$, sonic flow, the system of equations is parabolic, with Eqs. D-8 and D-10 having one real root and one characteristic direction at each point.

For the case $V > a$, Eq. D-8 defines two characteristic directions in the physical (x,y) plane

$$\left(\frac{dy}{dx}\right)_I = \frac{-uv - a\sqrt{V^2 - a^2}}{a^2 - u^2} \qquad \text{(D-11a)}$$

which has a positive angle with the streamline flow direction, and

$$\left(\frac{dy}{dx}\right)_{II} = \frac{-uv + a\sqrt{V^2 - a^2}}{a^2 - u^2} \qquad \text{(D-11b)}$$

having a negative angle with the streamline flow direction. Equation D-10 defines the corresponding pair of hodograph characteristics

$$\left(\frac{du}{dv}\right)_{I} = \frac{uv - a\sqrt{V^2 - a^2}}{a^2 - u^2} \quad , \qquad \text{(D-12a)}$$

and

$$\left(\frac{du}{dv}\right)_{II} = \frac{uv + a\sqrt{V^2 - a^2}}{a^2 - u^2} \qquad \text{(D-12b)}$$

in the (u,v) plane.

Using Eqs. D-11 and D-12, it is seen that

$$\left(\frac{dy}{dx}\right)_{I}\left(\frac{dv}{du}\right)_{II} = -1; \quad \left(\frac{dy}{dx}\right)_{II}\left(\frac{dv}{du}\right)_{I} = -1 \qquad \text{(D-13)}$$

which shows the system of characteristics is orthogonal.

If, in Fig. D-1, θ represents the inclination of the velocity vector V, and φ the direction of the characteristic with respect to the x-axis, then

$$u = V\cos\theta, \quad v = V\sin\theta \quad , \qquad \text{(D-14)}$$

$$\frac{dx}{ds} = \cos\varphi, \quad \text{and} \quad \frac{dy}{ds} = \sin\varphi \quad .$$

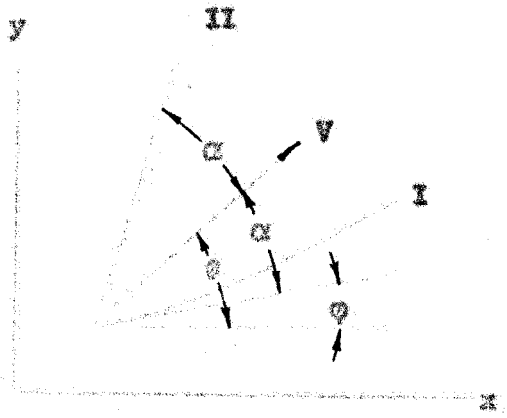

FIGURE D-1

Geometry of Physical Characteristics

Introducing Eq. D-14 into Eq. D-8 gives

$$a^2 = V^2 \sin^2 (\theta - \varphi) \quad , \tag{D-15}$$

or

$$(\theta - \varphi) = \sin^{-1} \frac{1}{M} = \alpha \quad ,$$

where α is the Mach angle. Therefore, the characteristic lines in the physical plane represent Mach lines, and the velocity vector bisects the angle between the characteristic lines, see Fig. D-1.

Since the equations of characteristics in the hodograph plane are independent of the initial conditions, the characteristic curves can be found by integration of Eq. D-9. Substituting

$$u = V \cos \theta, \qquad du = dV \cos \theta - V \sin \theta \, d\theta \quad ,$$

and

$$v = V \sin \theta, \text{ and } dv = dV \sin \theta + V \cos \theta \, d\theta$$

in Eq. D-9 gives

$$d\theta = \frac{1 + \tan\theta \tan(\theta \pm \alpha)}{\tan\theta - \tan(\theta \pm \alpha)} \frac{dV}{V}$$

$$= \pm \cot\alpha \frac{dv}{V} = \pm \sqrt{M^2 - 1} \frac{dV}{V} \qquad \text{(D-16)}$$

Using the relations

$$M = \frac{V}{a} \quad ,$$

$$a^2 = \gamma RT \quad ,$$

and

$$\frac{T}{T_o} = 1 + \frac{\gamma - 1}{2} M^2$$

Eq. D-16 can be expressed as

$$d\theta = \pm \frac{\sqrt{M^2 - 1}}{(1 + \frac{\gamma - 1}{2} M^2)} \frac{dM}{M} \qquad \text{(D-17)}$$

which upon integration gives

$$\pm \theta = \cos^{-1} \frac{1}{M} - \left(\frac{\gamma + 1}{\gamma - 1}\right)^{1/2} \tan^{-1} \left[\frac{\gamma - 1}{\gamma + 1}(M^2 - 1)\right]^{1/2} + c \qquad \text{(D-18)}$$

If solutions are required for a large number of initial conditions, it is more convenient to express Eq. D-18 in terms of $M^* = V/a^*$ rather than the Mach number M. Using the relation

$$M^2 = \frac{2}{\gamma + 1} M^{*2} / \left(1 - \frac{\gamma - 1}{\gamma + 1} M^{*2}\right) \quad ,$$

Eq. D-18 becomes

$$\pm \theta = \cos^{-1}\left(\frac{\gamma+1 - (\gamma-1)\,M^{*2}}{2\,M^{*2}}\right)^{1/2} -$$

$$- \left(\frac{\gamma+1}{\gamma-1}\right)^{1/2} \tan^{-1}\left(\frac{M^{*2} - 1}{1 - \frac{\gamma - 1}{\gamma + 1} M^{*2}}\right)^{1/2} + C \qquad \text{(D-19)}$$

Equations D-18 and D-19 represent epicycloids in the u,v plane originating at a point on the sonic circle generated by a circle with a diameter equal to $u_{max} - a_*$ if Eq. D-18 is used and $M_{max}^* - 1$ for Eq. D-19.

The sign of θ is taken to be positive when left running waves are considered and negative for right running waves. Then, for left running waves, Eq. D-15 can be expressed as

$$\theta + \omega = C_1 \quad , \qquad \text{(D-20)}$$

and for right running waves

$$\theta - \omega = - C_2 \quad , \qquad \text{(D-21)}$$

where the value of C_1 or C_2 represents the angle between a line from the origin to the starting point of the epicycloid curve and the u axis, and ω is the Prandtl-Meyer angle given by

$$\omega = \cos^{-1}\frac{1}{M} - \left(\frac{\gamma+1}{\gamma-1}\right)^{1/2} \tan^{-1}\left[\frac{\gamma-1}{\gamma+1}(M^2 - 1)\right]^{1/2} \qquad \text{(D-22)}$$

By addition and subtraction of Eqs. D-20 and D-21 the following relations are obtained

$$\theta = \frac{C_1 - C_2}{2} = a - b \quad , \tag{D-23}$$

and

$$\omega = \frac{C_1 + C_2}{2} = a + b \quad . \tag{D-24}$$

From Eq. D-24 it is seen that the flow velocity is determined by the sum of the constants a, b. If a is increased and b is decreased by the same amount the point described will move along a radius V = constant representing velocities of the same magnitude but different flow direction. The flow direction, given by Eq. D-23, is a function of the difference a - b. Thus, if a and b are changed by the same amount, the point described will move along a radial line θ = constant.

If the constant a is increased by an amount $+ \Delta \theta$ the flow is deflected through an angle $+ \Delta \theta$, and if be is increased by $+ \Delta \theta$ the flow is deflected through an angle $- \Delta \theta$. Therefore, if the flow crosses left running waves b is increased by an amount $\Delta \theta$ and a is unchanged, and when the flow crosses right running waves a is increased by $\Delta \theta$ and b is unchanged. Using this procedure, it is possible to solve supersonic flow problems by a semi-graphical method where the graphical construction is necessary in the physical (x,y) plane only.

Tunnel Section	Fig. No.	Part No.	No. Read
Entrance	8	1	1
		2	1
	9	1	1
		2	1
Nozzle	6	1	1
		2	1
	7	1	2
Test	10	1	2
		1	1
	15	2	1
		3	1
	16	1	1
		2	1
	17	1	1
		2	1
Model Mount	11	1	1
	12	1	1
	13	1	1
		2	1
		3	1
		4	2
		5	1
		6	1
		7	1

Tunnel Components

TABLE 1

Table 1 Continued.

Tunnel Section	Fig. No.	Part No.	No. Read
Diffuser	14	1	2
	17	3	2
		4	2
		5	2
	18	1	1
		2	2
		3	2
		4	1
		5	1
		6	2
		7	4

Tunnel Components

Table 1

M = 1.5028		M = 2.0585		M = 2.5372		M = 2.9105		M = 3.5937	
R_1	R_2	R_1	R_2	R_1	R_2	R_1	R_2	R_1	R_2
5.857	9.000	3.545	7.600	6.513	4.500	4.285	3.500	2.350	1.750
L_1	L_2	L_1	L_2	L_1	L_2	L_1	L_2	L_1	L_2
2.750	6.320	4.000	8.330	4.750	9.250	4.250	9.750	3.146	10.854
X	Y	X	Y	X	Y	X	Y	X	Y
0.000	1.443	0.000	0.958	0.000	0.632	0.000	0.438	0.000	0.229
0.162	1.445	0.200	0.960	0.100	0.634	0.051	0.440	0.032	0.232
0.610	1.450	0.400	0.965	0.200	0.641	0.105	0.444	0.064	0.234
Straight Line		0.600	0.981	0.300	0.650	0.185	0.453	0.094	0.237
3.780	1.610	0.785	1.000	0.400	0.661	0.272	0.462	0.123	0.241
4.000	1.625	Straight Line		0.500	0.672	0.378	0.482	0.151	0.248
5.000	1.670	3.781	1.370	Straight Line		Straight Line		0.176	0.251
6.000	1.690	4.000	1.400	3.525	1.210	3.000	1.036	0.207	0.260
6.320	1.700	5.000	1.515	4.000	1.270	4.000	1.210	Straight Line	
		6.000	1.600	5.000	1.405	5.000	1.365	2.192	0.795
		7.000	1.652	6.000	1.510	6.000	1.480	3.000	0.980
		8.000	1.690	7.000	1.595	7.000	1.572	4.000	1.170
		8.330	1.700	8.000	1.650	8.000	1.634	5.000	1.325
				9.000	1.690	9.000	1.685	6.000	1.450
				9.250	1.700	9.750	1.700	7.000	1.540
								8.000	1.610
								9.000	1.665
								10.000	1.690
								10.854	1.700

Coordinates for Nozzle Blocks
(Refer to Fig. 6)

TABLE 2

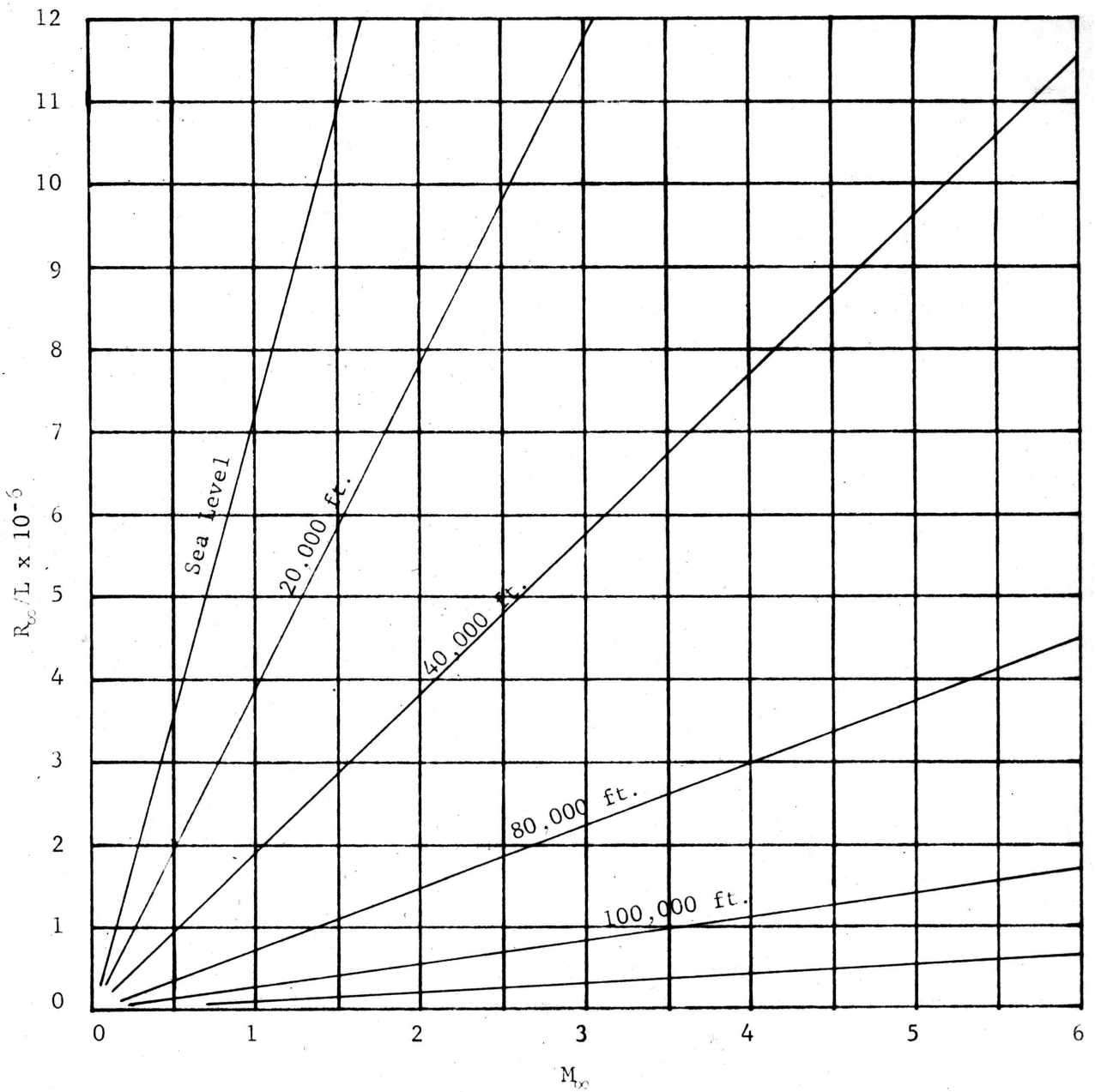

Variation of Reynolds Number with Altitude and Mach Number

FIGURE 1

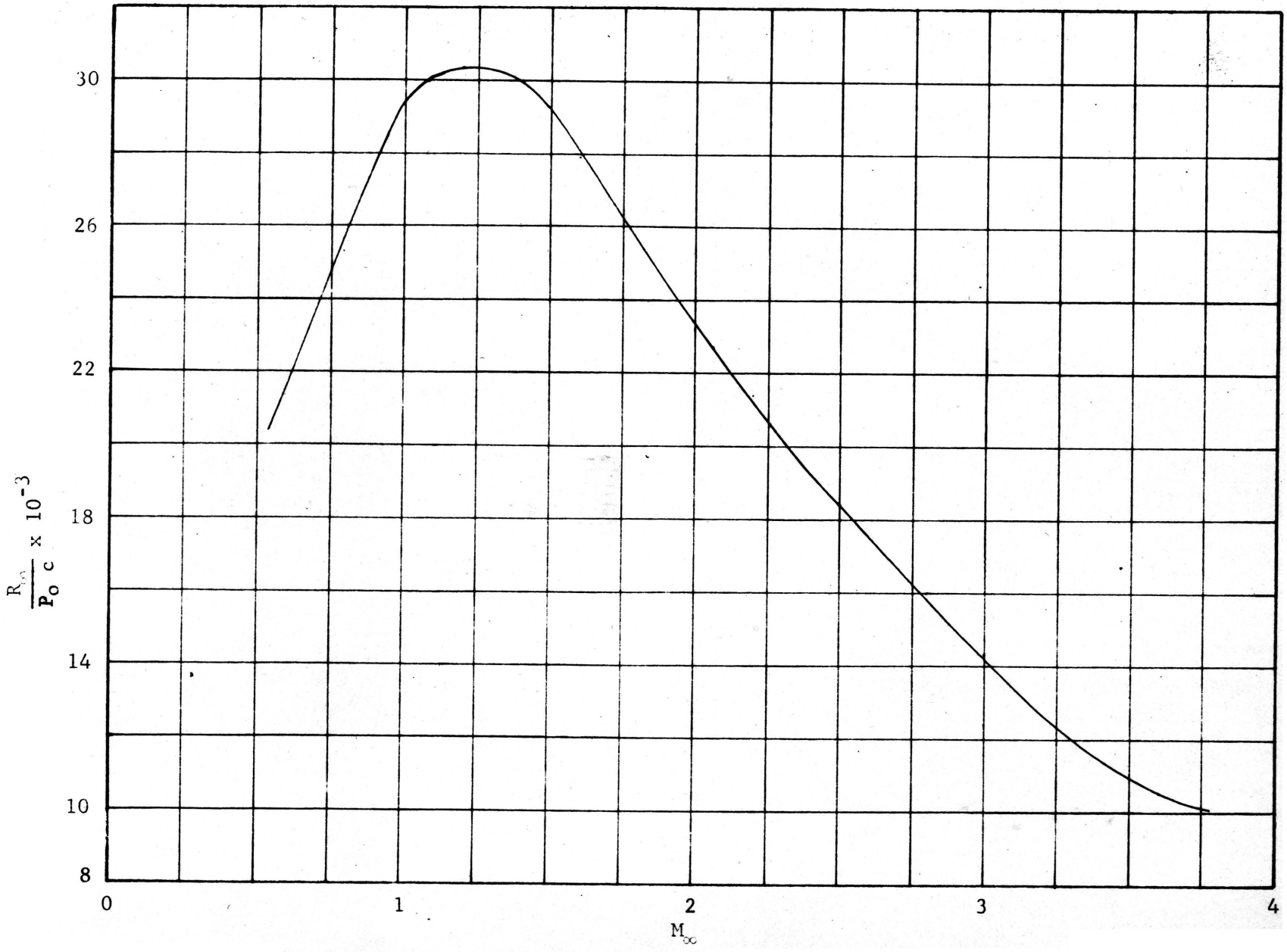

Variation of Test Reynolds Number with Mach Number for $T_o = 60^oF$

FIGURE 2

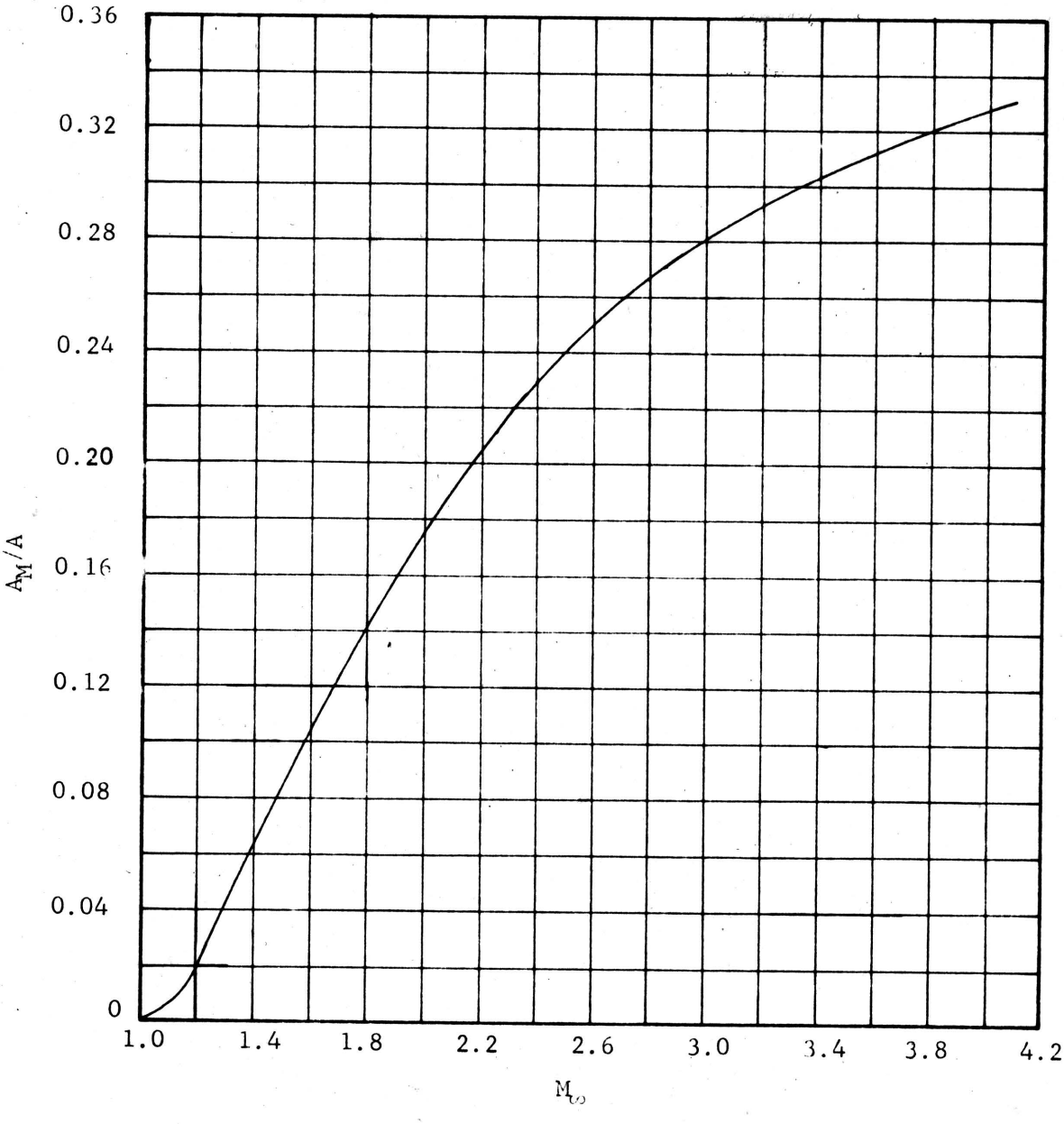

Variation of Maximum Permissible Model Cross-Sectional Area with Mach Number

FIGURE 3

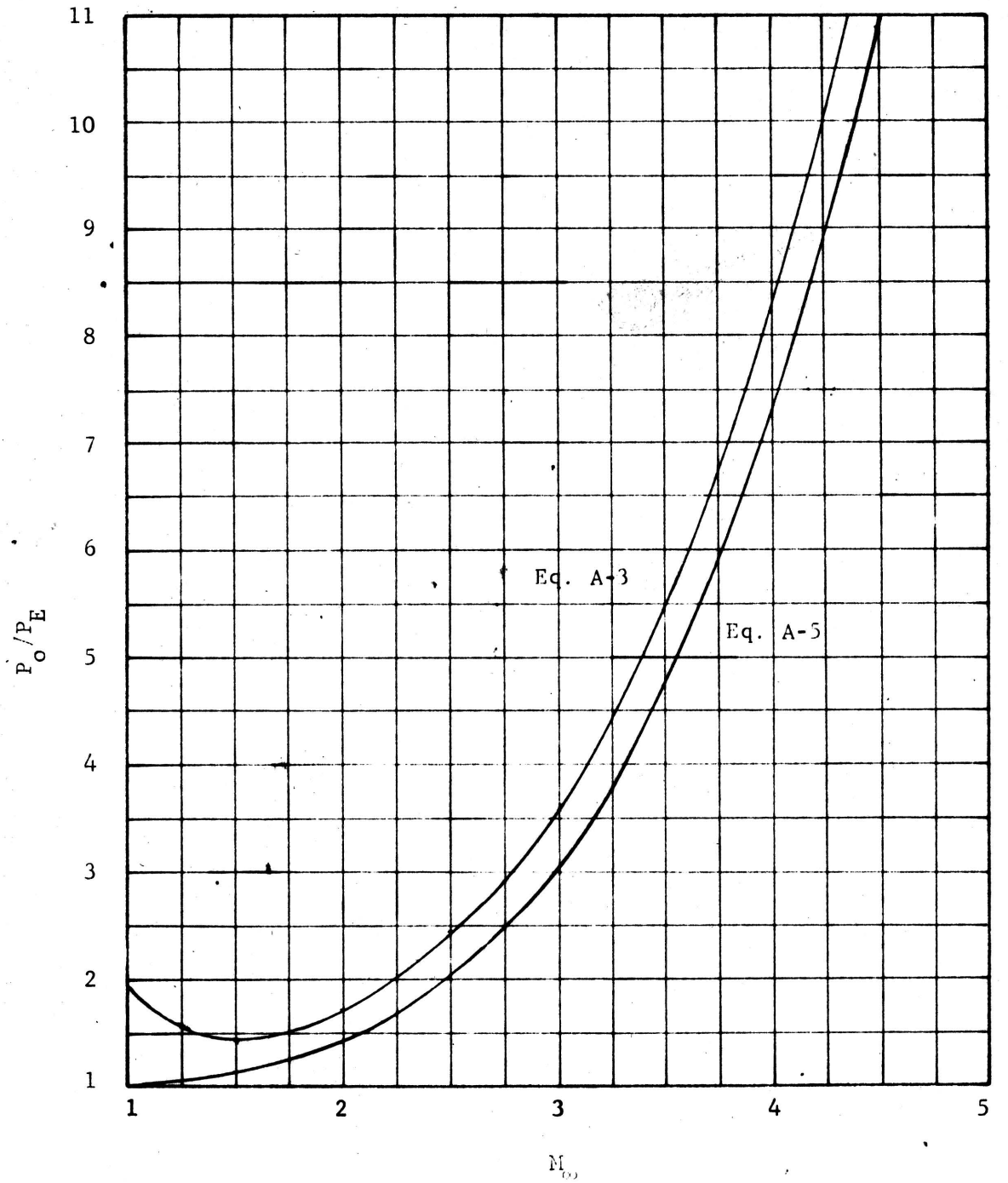

Pressure Ratio Variation with Mach Number

FIGURE 4

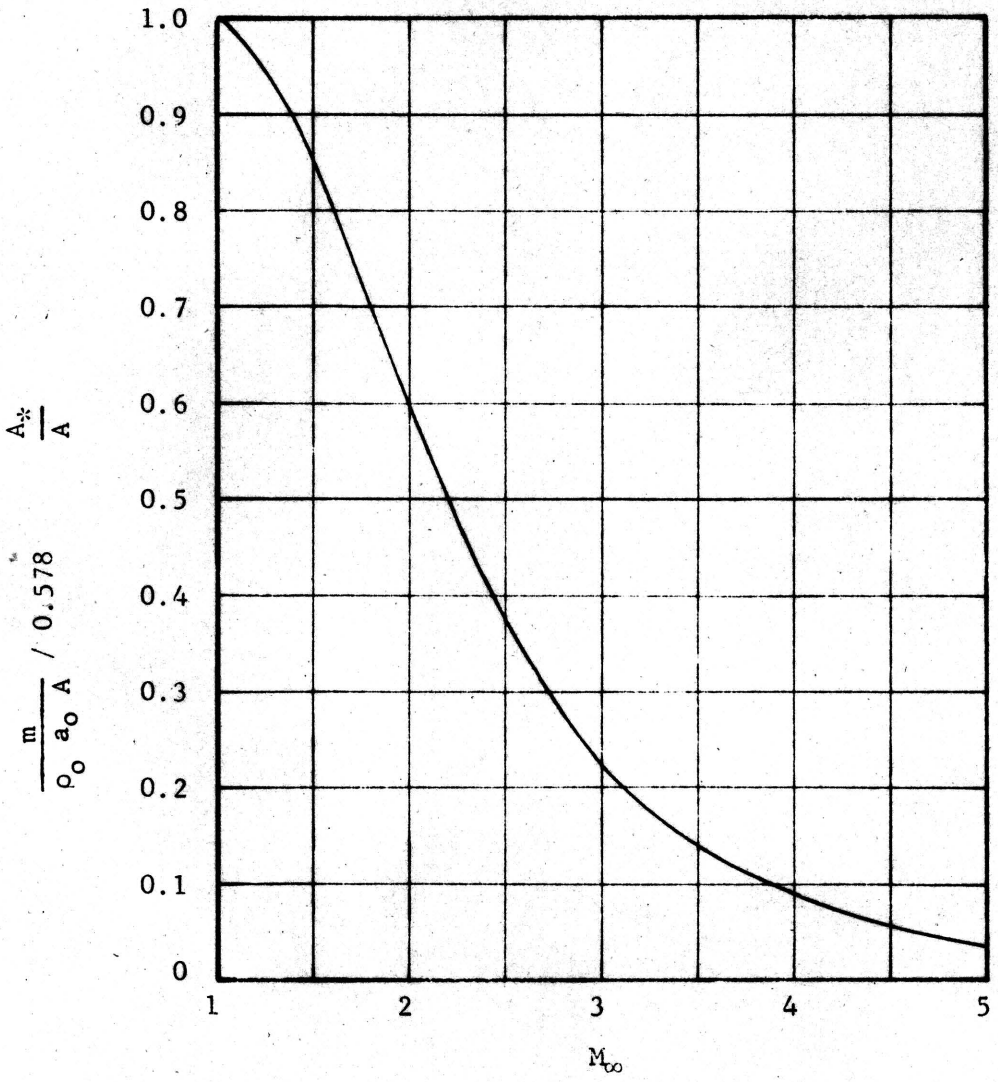

Variation of Mass Flow and Nozzle Throat - Exit Area Ratio with Mach Number

FIGURE 5

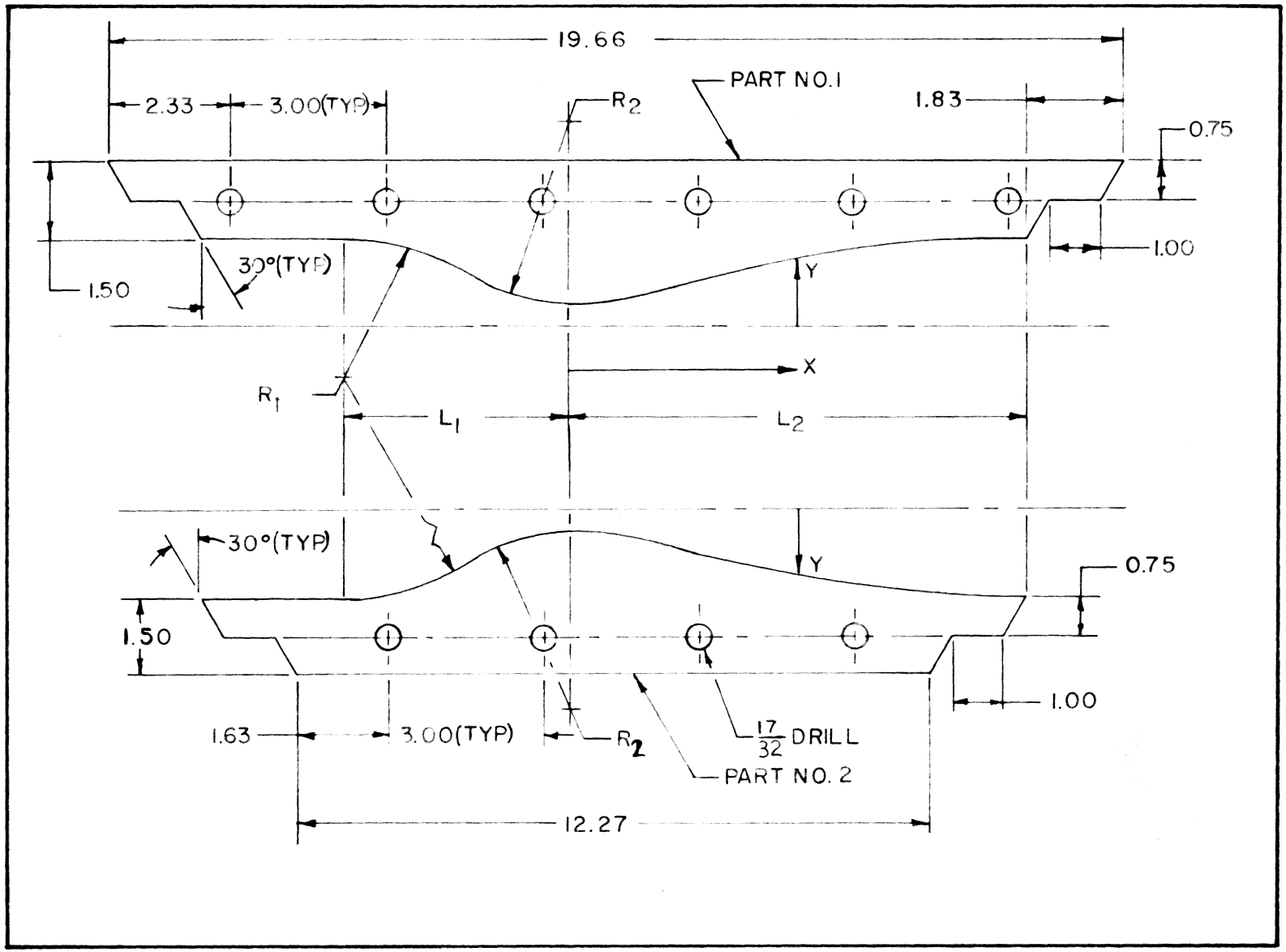

Nozzle Blocks

FIGURE 6

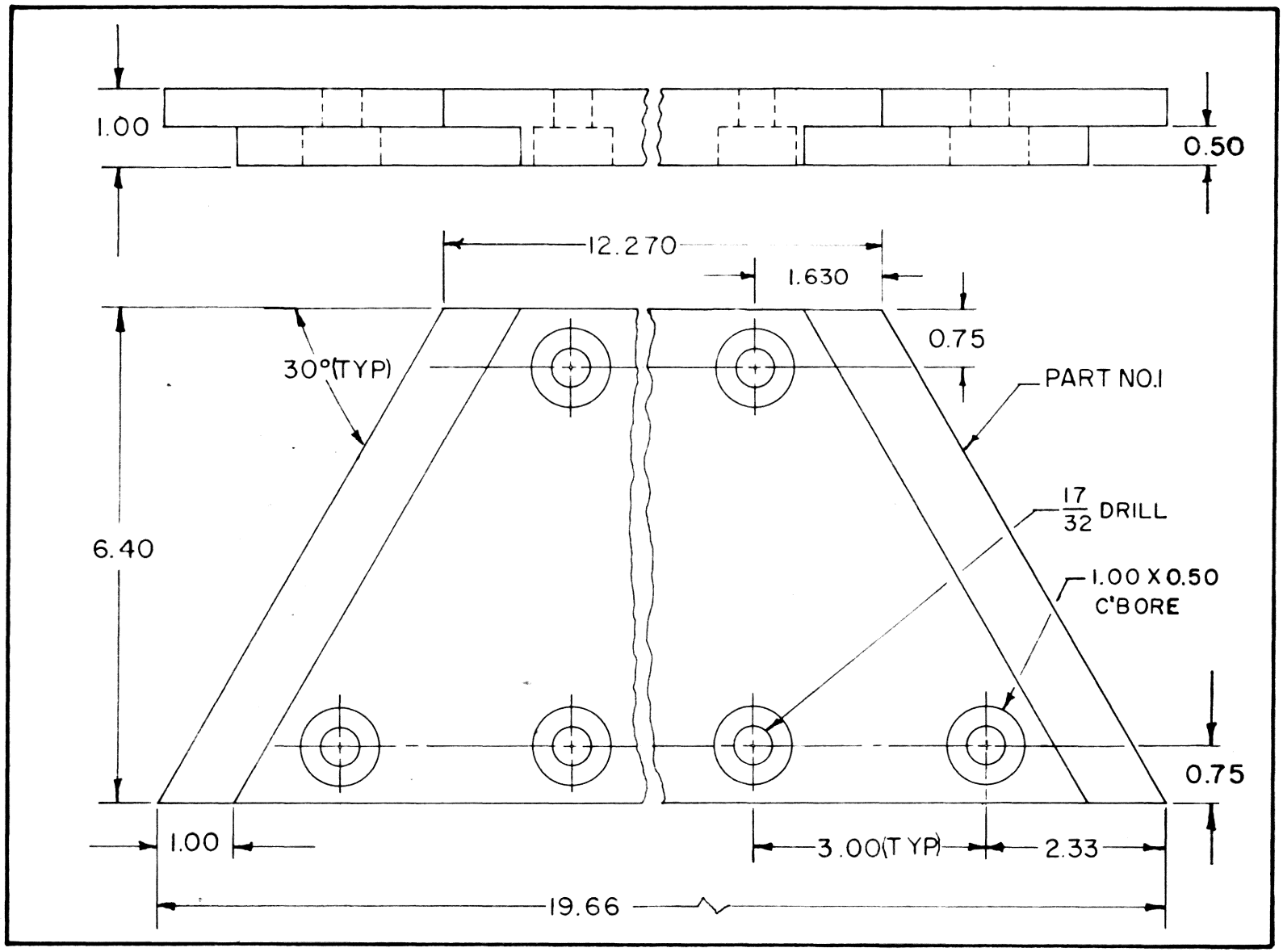

Nozzle Wall

FIGURE 7

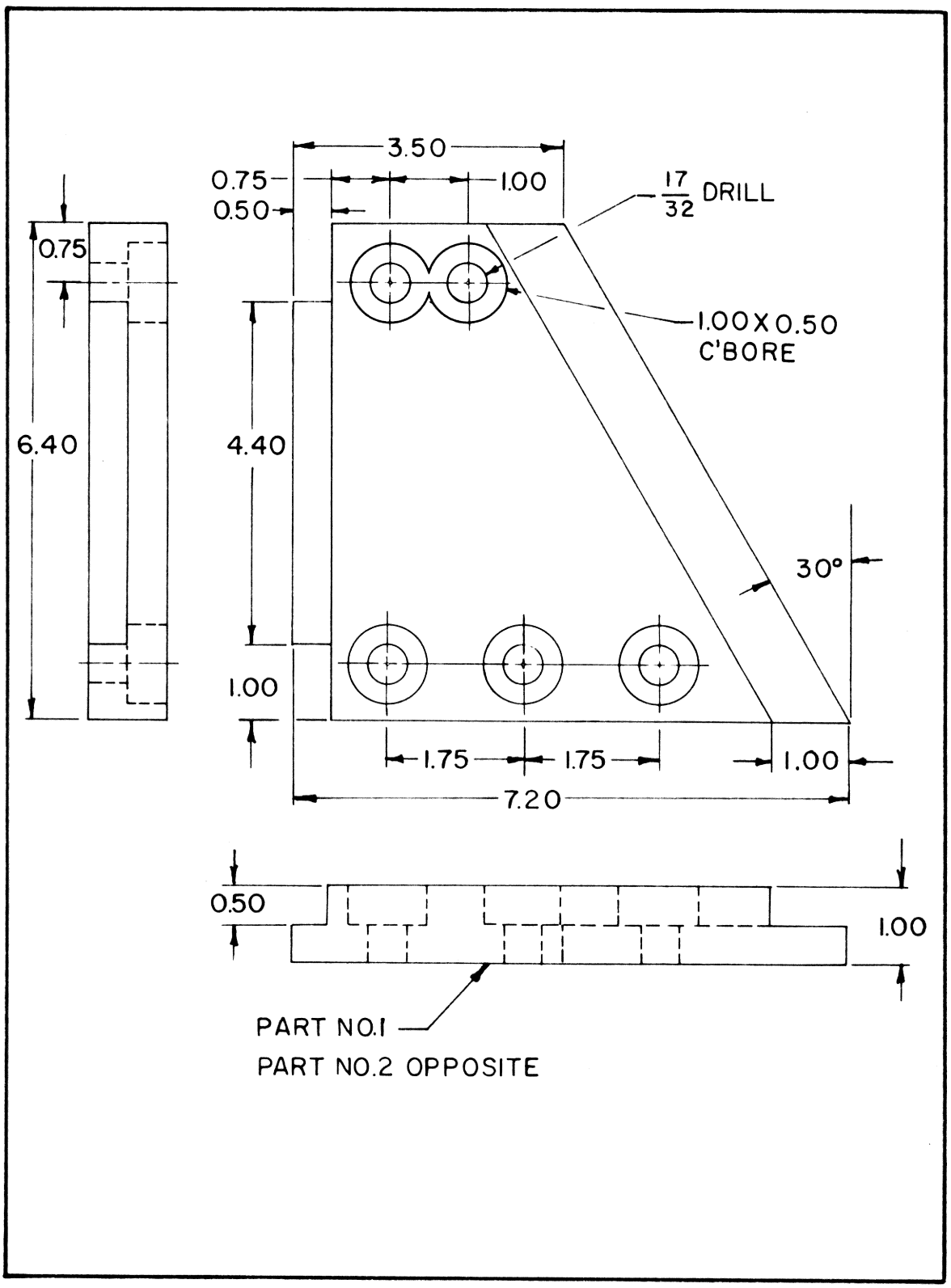

Entrance Section Wall

FIGURE 8

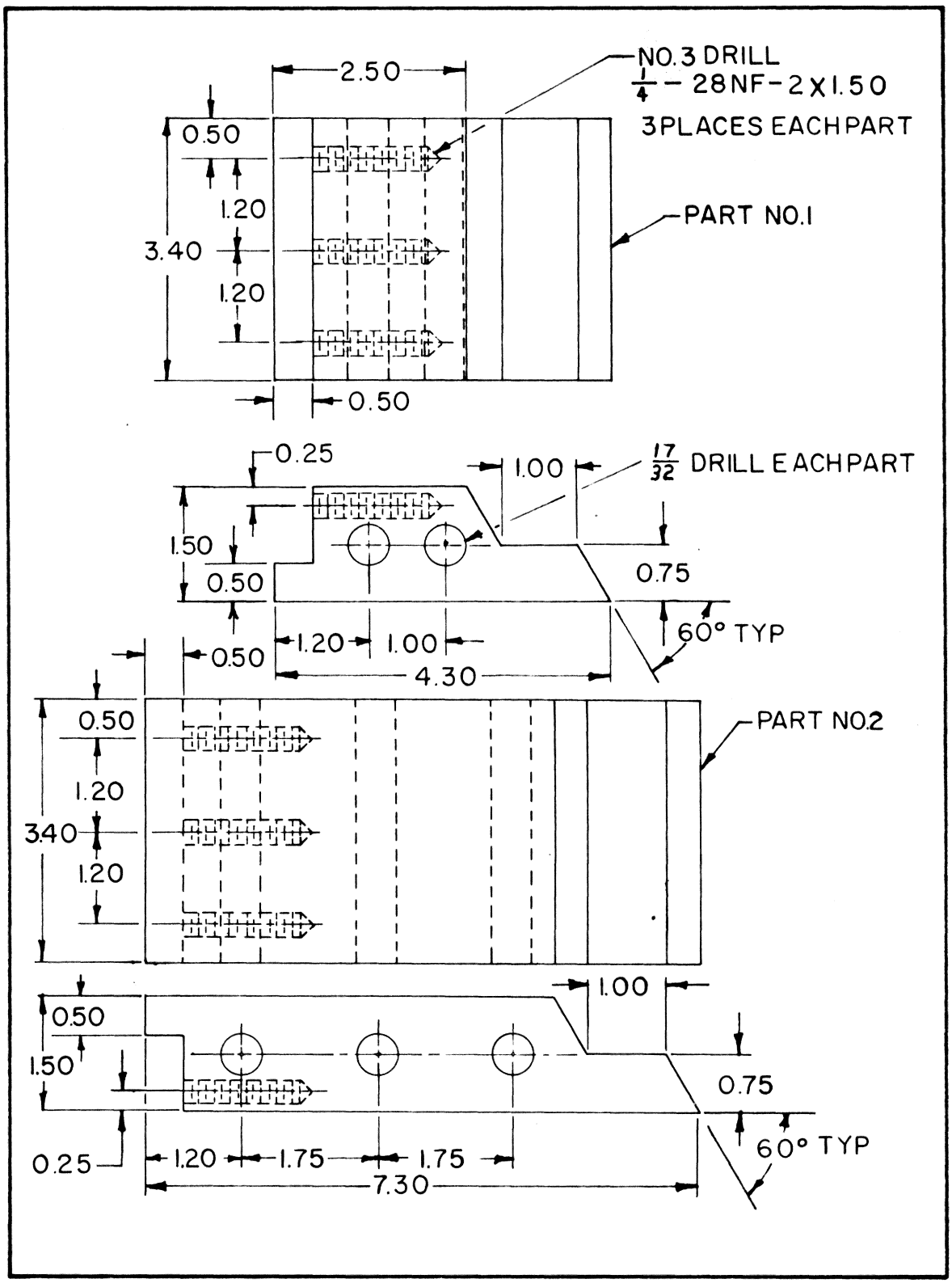

Entrance Section Floor and Ceiling

FIGURE 9

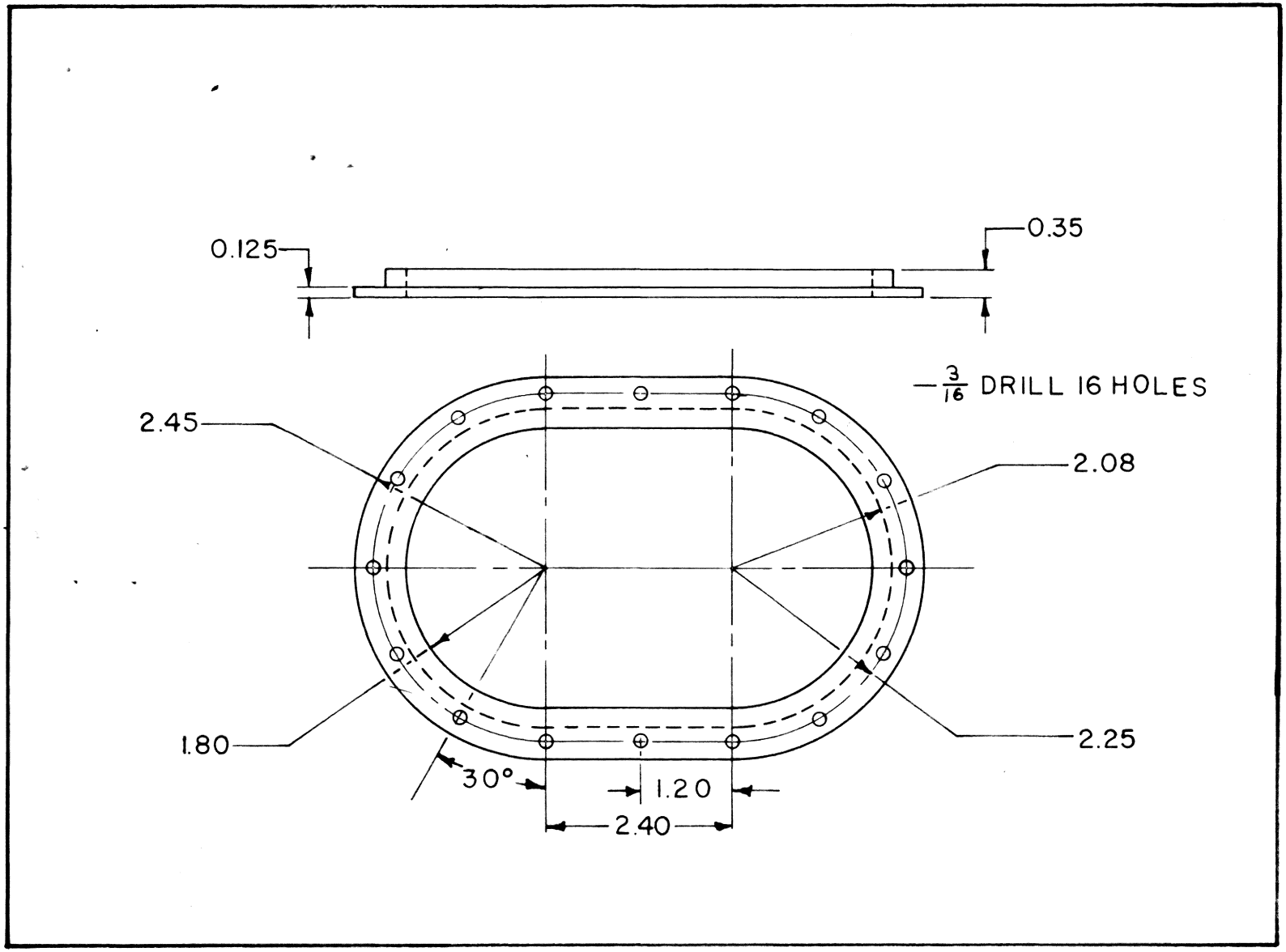

Retainer Ring

FIGURE 10

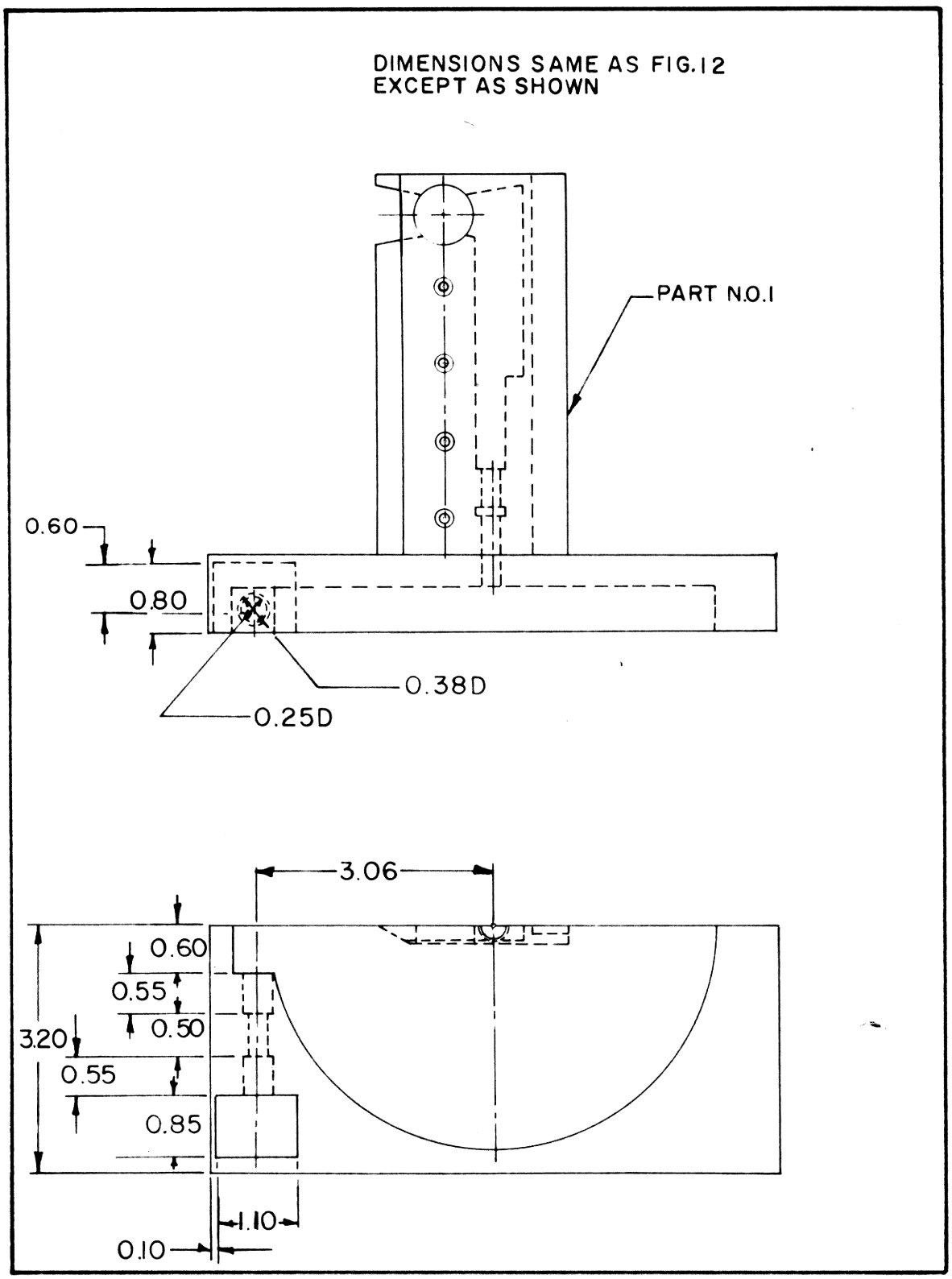

Model Mount Left Hand Side

FIGURE 11

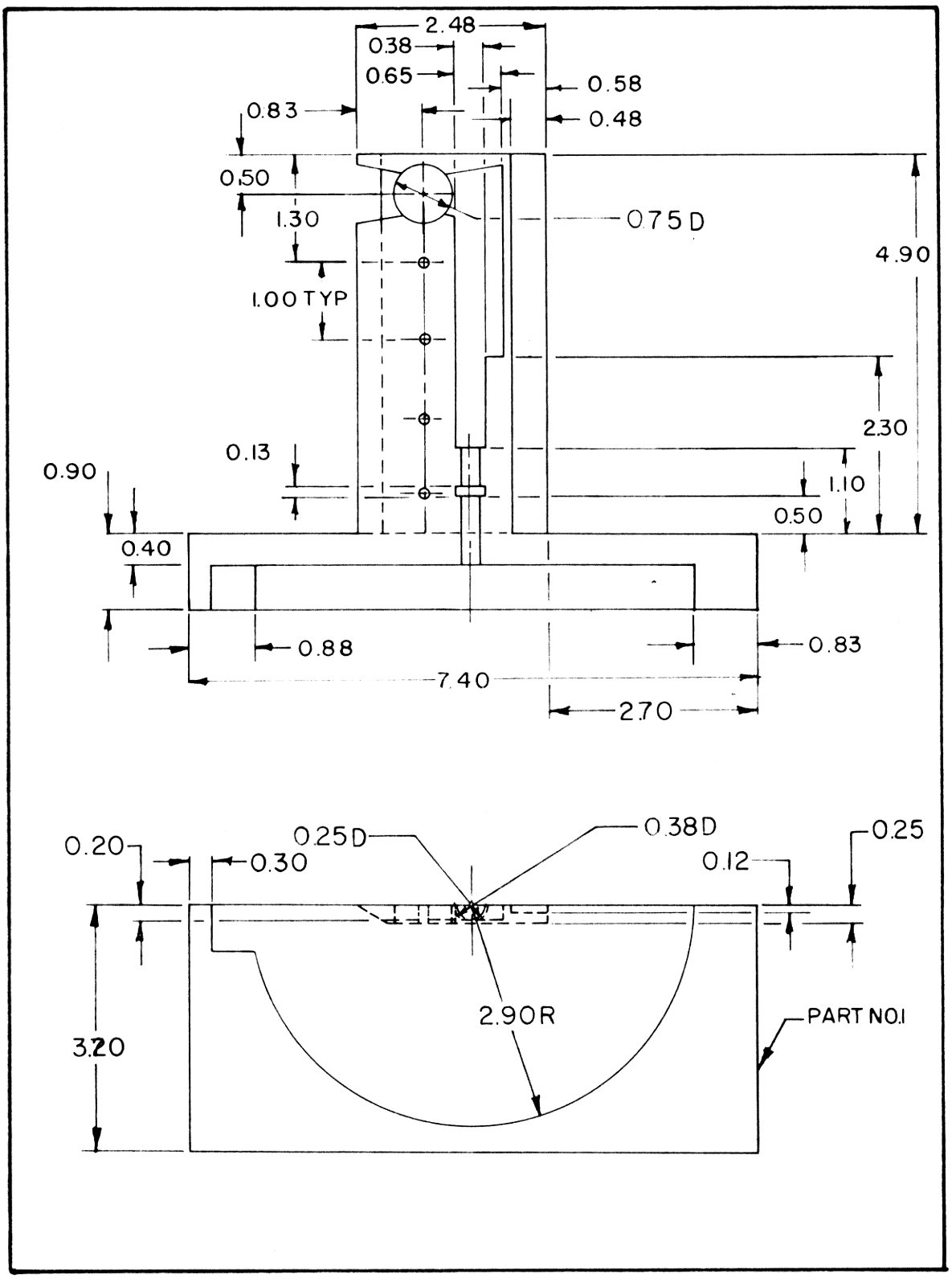

Model Mount Right Hand Side

FIGURE 12

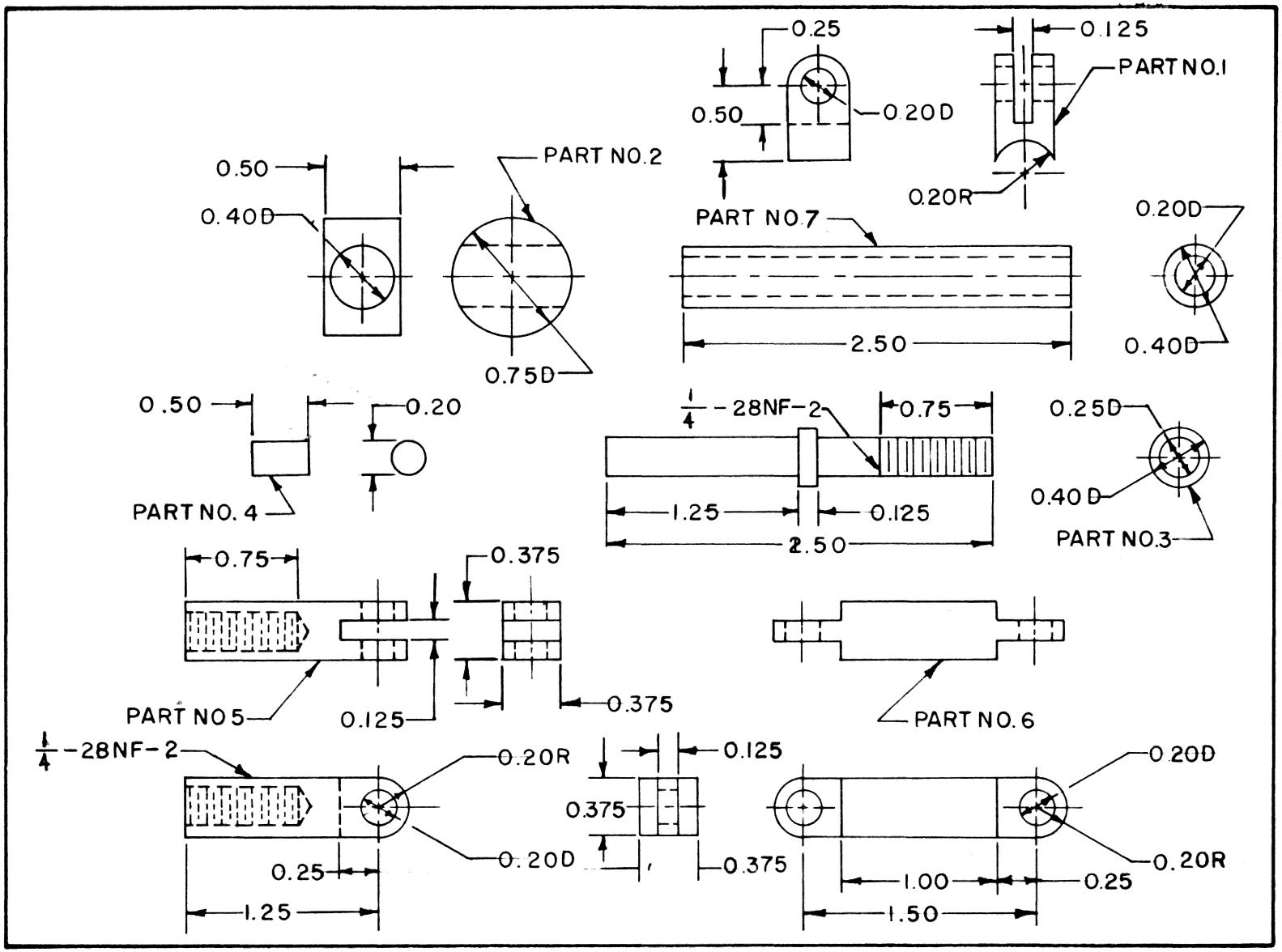

Model Mount Linkages

FIGURE 13

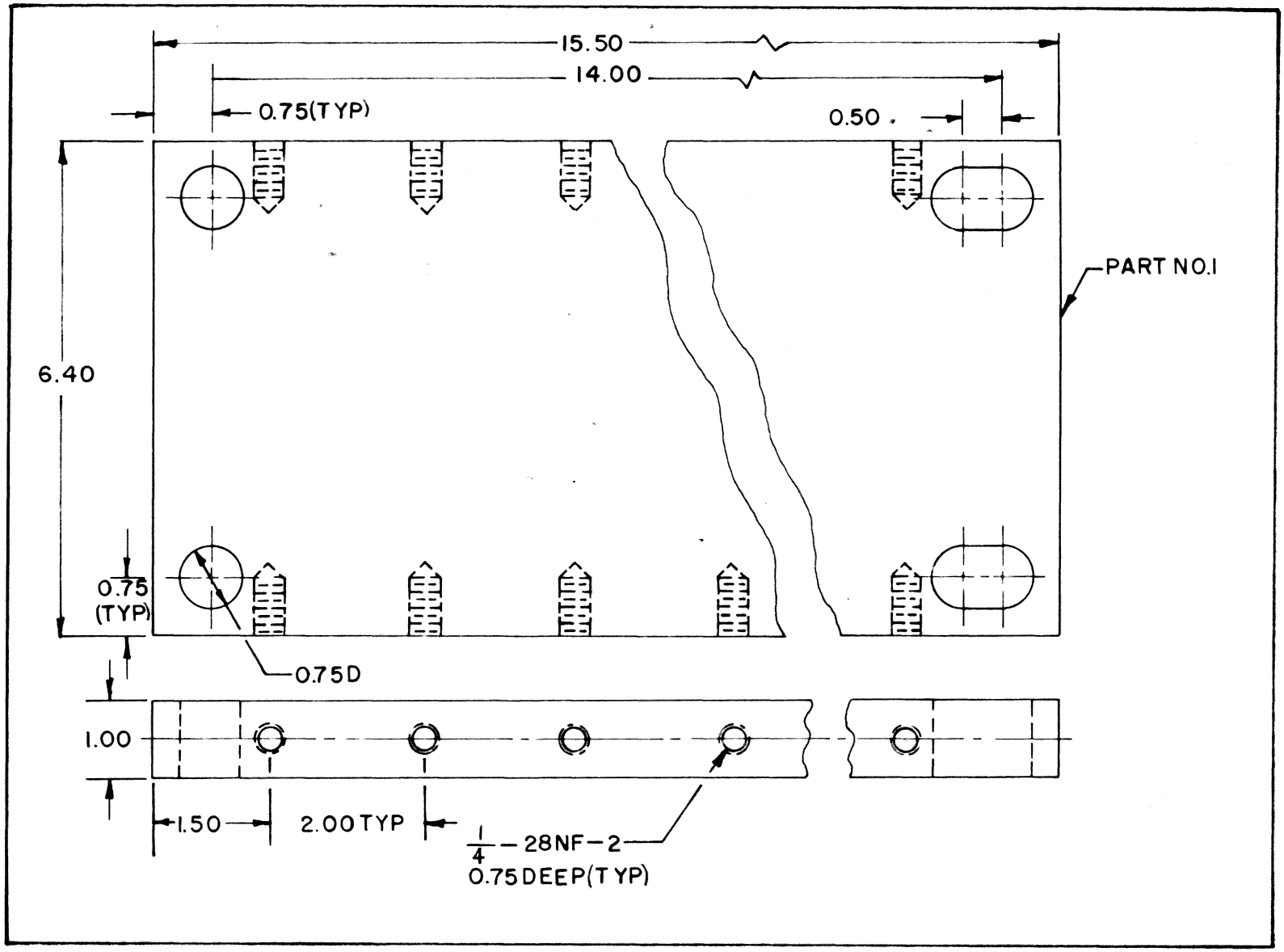

Diffuser Sidewall

FIGURE 14

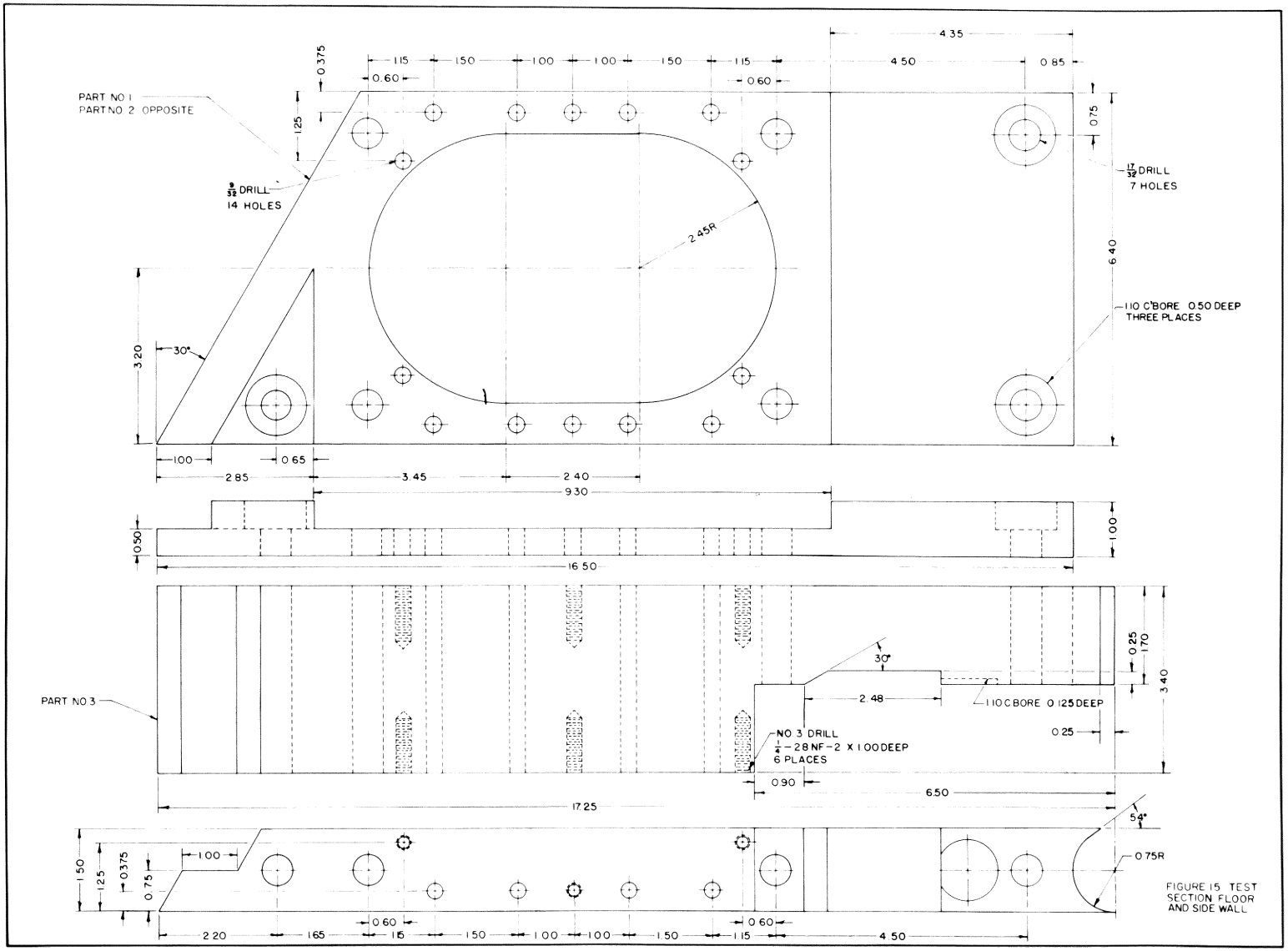

FIGURE 15 TEST SECTION FLOOR AND SIDE WALL

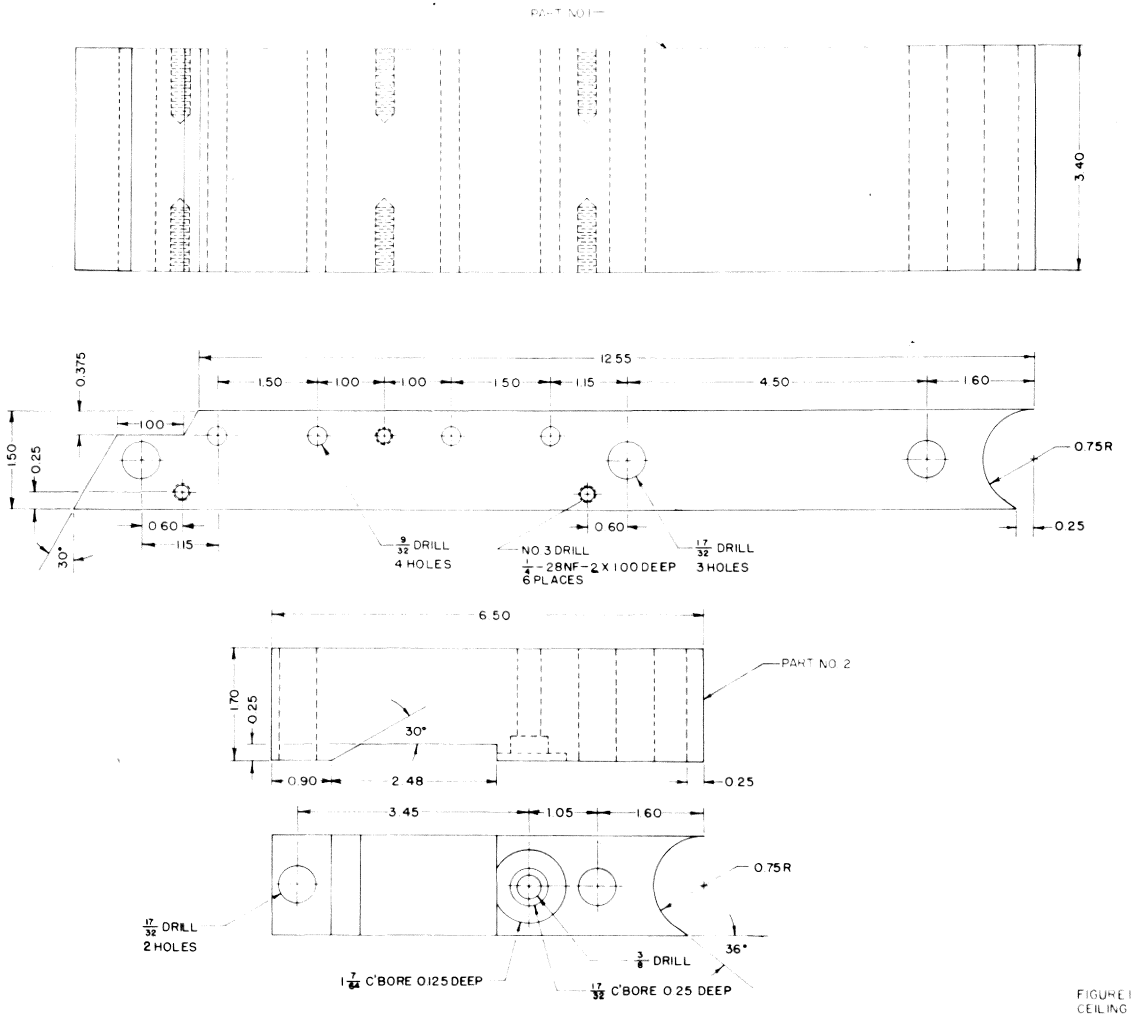

FIGURE 16 TEST SECTION
CEILING AND FLOOR

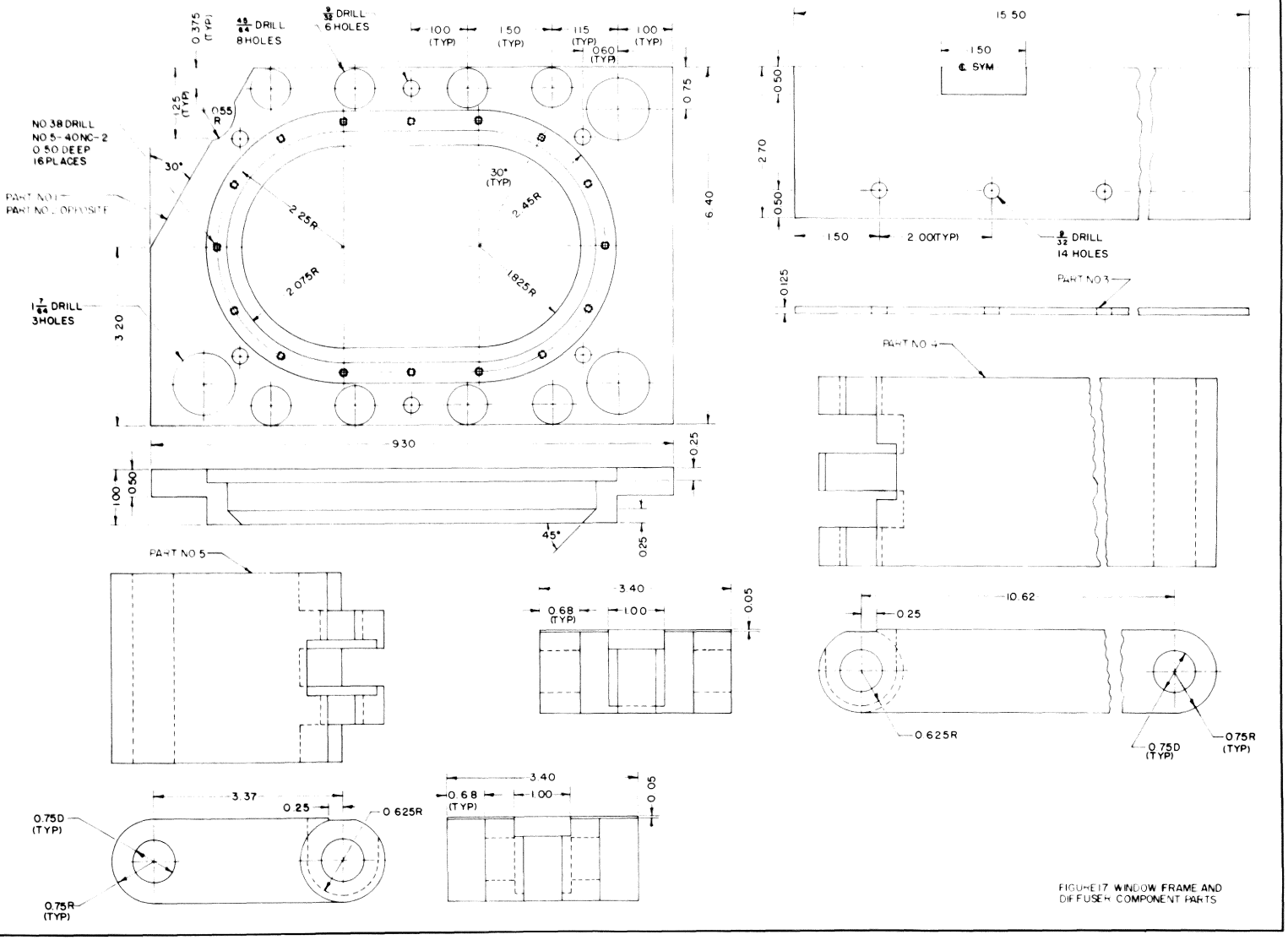

FIGURE17 WINDOW FRAME AND DIFFUSER COMPONENT PARTS

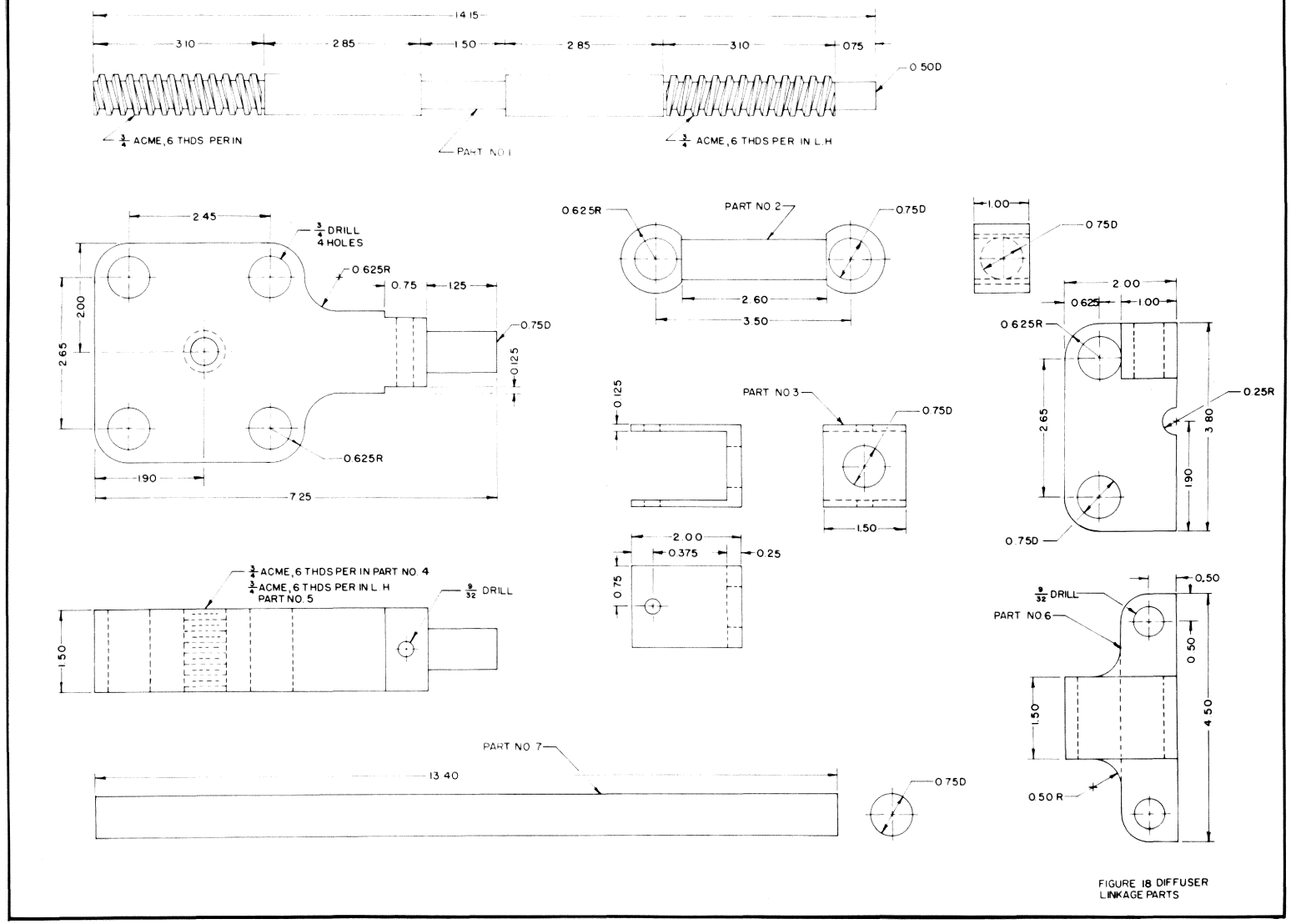

FIGURE 18 DIFFUSER LINKAGE PARTS

THE DESIGN OF A 3.4 BY 3.4 INCH SUPERSONIC WIND TUNNEL CAPABLE OF CONTINUOUS OPERATION IN THE RANGE OF MACH NUMBERS BETWEEN 1.50 AND 3.59

by

E. C. Anderson

ABSTRACT

The design of a continuous flow supersonic blow down wind tunnel suitable for student instruction and basic research is described. The wind tunnel is capable of operation in the supersonic range of Mach numbers from 1.50 to 3.59 and Reynolds numbers from 1.1×10^6 to 5.0×10^6 are obtained. The design procedures outlined are applicable to all types of supersonic wind tunnels.